Dottorato di Ricerca in Biologia Cellulare e Molecolare

Dipartimento di Biotecnologie e Scienze della Vita
Università degli Studi dell'Insubria

Degeneration of the larval midgut of *Bombyx mori* during metamorphosis: role and regulation of autophagy and apoptosis

Tesi di Dottorato di Davide Romanelli

Tutor: Prof. Gianluca Tettamanti

Anno Accademico 2014/2015

INDEX

ABSTRACT

The midgut of the silkworm, *Bombyx mori*, is extensively remodeled during metamorphosis: in fact, while cell death processes lead to the degeneration of the larval epithelium, the adult midgut is formed by the proliferation and differentiation of stem cells. Our group previously described the intervention of apoptotic and autophagic events in larval midgut cells undergoing degeneration (Franzetti et al., 2012). The present study aims at investigating the molecular pathways of apoptosis and autophagy, the role of the two processes and their relationship in this tissue.

We first analyzed the expression pattern of autophagic and apoptotic genes, as well as used specific markers to assess the precise timing of autophagy and apoptosis during metamorphosis. The results obtained confirm that autophagy is activated at spinning stage, while apoptosis intervenes with a delay of 24-48 hours. The final demise of apoptotic cells occurs by secondary necrosis and their content is released in the lumen of the adult midgut.

To investigate the mechanisms that lead to the activation of autophagy and apoptosis we used 20-hydroxyecdysone (20E), one of the main regulators of metamorphosis in insects. The administration of a single dose of 20E induces the transcription of both autophagic and apoptotic genes, but fully activates only autophagy. In contrast, the activation of effector caspases needs a second injection of 20E. These data suggest that, during development, autophagy is induced at the end of the last larval stage by the 20E commitment peak, while the onset of apoptosis occurs concomitantly with 20E metamorphic peak. Moreover, our results demonstrate that 20E activates autophagy by inhibiting the Tor pathway. However, inactivation of Torc1 through rapamycin administration is not sufficient to trigger and maintain a full

autophagic response, thus suggesting that the activation of autophagy by 20E is mediated by multiple downstream targets.

In order to study the role of autophagy and apoptosis in this setting we used specific inhibitors. The impairment of the autophagic flux, through administration of chloroquine, determines an increased degeneration of the larval midgut epithelium and higher levels of caspase activity compared to controls, while the inhibition of caspase activation, by using z.vad.fmk, leads to a severe delay in the degradation of the epithelium. These data demonstrate that, while autophagy has a pro-survival role in this setting, apoptosis is the major process that drives the demise of the larval midgut during metamorphosis.

1 INTRODUCTION

1.1 Metamorphosis and hormonal regulation of development in insects

Metamorphosis is a process that allows the morphological modification of the different life stages of a certain species, allowing the organism to exploit different habitats and food sources. Insects that belong to the most primitive orders show direct development (ametabolous insects) and their juvenile stage looks very much like the adult, except for the lack of functional genitalia. Ametabolous insects include the bristletails and the silverfish. In insects with "incomplete" metamorphosis (hemimetabolous insects) the immature stage (nymph) lacks genitalia and, in winged species, the nymph bears wing buds which are transformed into functional wings during the moult to the adult stage. Hemimetabolous insects include cockroaches, grasshoppers and dragonflies. Insects with "complete metamorphosis" (holometabolous insects) are characterized by different larval, pupal and adult stages, thus allowing a different use of the resources needed for growth and reproduction. Holometabolous insects include beetles, flies, moths and bees (Truman and Riddiford, 1999). We will use hereafter the term metamorphosis referring to complete metamorphosis. During this process the external and internal body structure is completely remodeled through processes of tissue degeneration and regeneration. These are finely regulated by hormonal cues. Three major classes of hormones control moulting and metamorphosis: the prothoracicotropic hormone (PTTH) (and other neuropeptides), the ecdysteroids, and the juvenile hormones (JHs). Neurosecretory cells localized in the brain secrete PTTH, which passes through nerve axons to the corpora cardiaca or the corpora allata. These

organs store and release PTTH into the haemolymph, starting each molt by stimulating the synthesis and secretion of ecdysteroid by the prothoracic glands. Production of ecdysteroids occurs in all insects: this group of hormones comprises ecdysone (E) and 20-hydroxyecdysone (20E). Ecdysone is released from the prothoracic glands into the hemolymph and is usually then converted to the more active 20E in several peripheral tissues, especially the fat body (Gullan and Cranston, 2014). E and 20E differ in their biological effects and the concentration of these two hormones in the hemolymph is important for the timing of developmental changes (Truman and Riddiford, 2002). The inactivation of 20E is achieved in two different ways: it can be irreversibly hydroxylated to 20,26-dihydroxyecdysone or sequestered in the form of 20E-phosphate and then excreted or stored for later use (Rees, 1995). JHs, on the other hand, are produced from the corpora allata and can be divided in different classes based on their structures. While JH-III is usually found in most insects, Lepidoptera rely on JH-I and JH-II (Roe and Venkatesh, 1990). JHs inhibit the expression of adult features so that a high hemolymph level of JHs is associated with a larval–larval moult, a lower concentration with a larval–pupal molt, while JHs are absent at the pupal–adult molt (Gullan and Cranston, 2014). The metabolic inactivation of JHs involves the modification of either the ester or the epoxide group (Roe and Venkatesh, 1990).

In Lepidoptera, most of the studies regarding the hormonal regulation of metamorphosis have been performed in *Manduca sexta*. In this species, during the final larval instar, JH titer declines to undetectable levels in both the hemolymph and tissues. A decrease in JH concentration allows the release of PTTH that consequently permits the release of ecdysone. A high concentration of ecdysone, in the absence of JH, leads to cessation of feeding and the onset of the wandering stage (20E commitment

peak). During the prepupal period JH increases and is necessary to prevent precocious metamorphosis in some tissues. JH decreases again during pupal ecdysis so that the subsequent ecdysteroids rise (metamorphic or pupal peak) occurs in the absence of JH and causes the metamorphosis to the adult stage (Truman and Riddiford, 2002) (Fig. 1). A similar regulation by hormones was described in the silkworm, *Bombyx mori* (Satake et al., 1998).

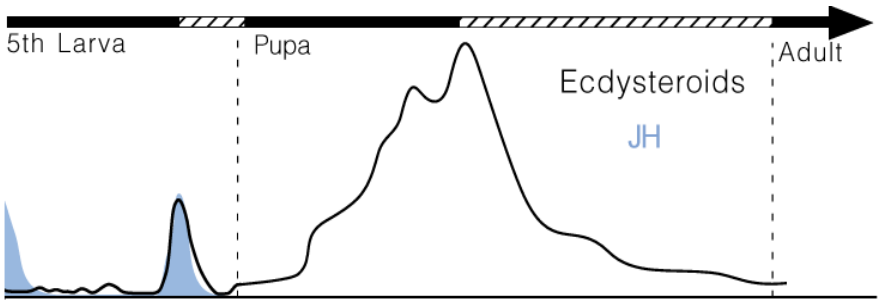

Figure 1 - Hormonal titers during Lepidoptera metamorphosis (modified from Truman and Riddiford, 1999).

The molecular basis of 20E activity is well studied in insects. 20E binds to the ecdysone nuclear receptor (EcR), which then interacts with the ultraspiracle protein (USP) to direct metamorphosis by mediating the expression of genes, including several transcription factors (Cai et al., 2014). In the 20E signalling pathway of the lepidopteron *B. mori*, EcR binds with USP to form a heterodimer, which can bind and regulate the expression of several key genes, such as *Broad complex* (*BR-C*), *E74 E75, HR3,* ßftz-F1 and E93 (Li et al., 2015; Liu X et al., 2015; Tian et al., 2013). In the JH signal transduction pathway, methoprene-tolerant (Met) proteins are regarded as potential candidate receptors for JH. In *B. mori*, Met2, one of the two Met isoforms, combines with steroid receptor co-activator (SRC) to form a heterodimer and induces the expression of downstream genes (Ou et al., 2014). In *B. mori* and other lepidopterons 20E is the inducer and regulator of processes related

to programmed cell death (PCD) in different organs such as the fat body (Tian et al., 2012; Tian et al., 2013) and the silk gland (Matsui et al., 2012; Sekimoto et al., 2006). On the other hand, JH seems to inhibit PCD in the same context (Matsui et al., 2012; Parthasarathy and Palli, 2007). The fine regulation of PCD processes by hormones is crucial for the correct reshaping of insect tissues during metamorphosis since cell death processes lead to the degeneration or the remodeling of larval organs that are no more needed during the pupal and adult stages.

1.2 Classification of cell death

Different classifications of the processes that lead to the demise of the cells have been proposed according to morphological appearance, enzymological criteria (absence or presence of nucleases or proteases), functional aspects (programmed or accidental, physiological or pathological) or immunological characteristics (immunogenic or non immunogenic) (Kroemer et al., 2009). In particular, several definitions of cell death, based on morphological criteria, can be found in the literature. Some of them define processes that are context-specific (e.g., cornification, mitotic catastrophe) or are related to pathologies, while others identify processes that can not be uniquely distinguishable from other cell death modalities (Galluzzi et al., 2012; Kroemer et al., 2009).

The three main cell death processes that have been observed and well characterized in most of the settings, including developmental processes, can be classified as (Fig. 2):

- **Type 1 cell death (apoptosis)** shows nuclear condensation and fragmentation, membrane blebbing and formation of apoptotic bodies that are later engulfed by

phagocytes. The activation of caspases is usually observed in apoptosis (Galluzzi et al., 2007, Kroemer et al., 2009);

- **Type 2 cell death (autophagic cell death)** is characterized by the presence of autophagosomes and autolysosomes in the cell cytoplasm (Kroemer et al., 2009). Autophagic cell death occurs in the absence of chromatin condensation and no intervention of phagocytes is observed (Klionsky et al., 2012). The occurrence of "autophagic cell death" has been described in some contexts based only on morphological features. However, in this case, the term must be simply considered as the direct observation of a cell that dies in the presence of autophagy. Functional studies are therefore needed to distinguish between "cell death by autophagy", where autophagy actively contributes to the process, from "cell death with autophagy", where it simply accompanies the cell death process without having an active role (Galluzzi et al., 2007; Kroemer et al., 2008);
- **Type 3 cell death (necrosis)** is characterized by an increase in cell volume, swelling of cytoplasmic organelles, membrane rupture, and release of cytoplasmic content in the extracellular environment. Necrosis is usually considered an uncontrolled form of cell death, but evidence accumulated in recent years shows that its execution may be finely regulated at least in some contexts. Therefore the term "necroptosis" has been proposed to indicate regulated necrosis (Galluzzi et al., 2007; Kroemer et al., 2009).

The morphological classification of cell death is based on the assumption that similar morphological features are due to the activation of similar cell death pathways. This type of classification is still very popular due to the easiness of use and to the presence of standardized and long-standing guidelines. On the contrary, in some instances, cell death phenotypes showing similar

morphologies can possess functional, biochemical and immunological heterogeneity. Moreover, the presence of specific morphological features is not usually sufficient to prove the existence of a causal link between a process and the observed cellular demise.

Cell death mode	Morphological features
Apoptosis	Rounding-up of the cell Retraction of pseudopodes Reduction of cellular and nuclear volume (pyknosis) Nuclear fragmentation (karyorrhexis) Minor modification of cytoplasmic organelles Plasma membrane blebbing Engulfment by resident phagocytes, *in vivo*
Autophagy	Lack of chromatin condensation Massive vacuolization of the cytoplasm Accumulation of (double-membraned) autophagic vacuoles Little or no uptake by phagocytic cells, *in vivo*
Necrosis	Cytoplasmic swelling (oncosis) Rupture of plasma membrane Swelling of cytoplasmic organelles Moderate chromatin condensation

Figure 2 - Main cell death modalities (adapted from Kroemer et al., 2009).

Information on the type of cell death that occurs in a given context can be also achieved by using biochemical or molecular methods. One of the advantages of these kinds of assays, in comparison to morphological observations, is that they are quantitative rather than qualitative. An exhaustive classification of cell death modalities based on biochemical features can be found in Galluzzi et al. (2012). However, these methods must be used and interpreted with caution, especially when a single cell death marker is considered (Galluzzi et al., 2012).

1.3 Apoptosis

The term "apoptosis" refers to a type of cell death that is accompanied by morphological features such as loss of the cell

morphology, reduction of volume (pyknosis), plasma membrane blebbing, nuclear condensation and fragmentation (karyorrhexis). Classical markers of apoptosis rely on the search for late apoptotic features such as caspase activation by using immunoblotting or immunohistochemistry, the TUNEL technique (Terminal deoxynucleotidyl transferase dUTP nick end labeling), assessment of DNA fragmentation by using electrophoresis, and morphological observation of condensed and fragmented nuclei by using light or electron microscopy. The term "apoptosis" should be used only when cell death events are accompanied by several of these morphological features. The apoptotic process usually ends *in vivo* with the engulfment by phagocytes (Kroemer et al., 2009). Under *in vitro* or *in vivo* conditions, where phagocytes are not present, apoptotic cells usually break up and release cytoplasmic components into the extracellular environment in a process called secondary necrosis (Silva, 2010).

In metazoans, apoptosis has a crucial role in maintaining the homeostasis of the organism and during its development. The deregulation of apoptosis in humans leads to a variety of pathologies including cancer, autoimmune diseases and neurodegenerative disorders (Riedl and Shi, 2004). During metazoan development the production of an excess of cells, followed by an apoptotic culling during later stages, allows to obtain the correct number and type of cells in different organs. The body structures are usually produced at early stages of development and later removed or reshaped by apoptosis, thus enabling primordial tissues to be adapted for different functions at different life stages or in different sexes. For instance, during early vertebrate development the pronephric kidney tubules arise but, although these structures form functional kidneys in fish and in amphibian larvae, they are useless and degenerate in mammals. Similarly, during insects and amphibian metamorphosis, apoptosis

eliminates tissues that are no longer useful, such as larval structures in insects or the amphibian tadpole tail (Meier et al., 2000).

From a genetic point of view, the basis of cell death in metazoans was first studied in the nematode *Caenorhabditis elegans*. In this experimental model four main proteins constitute the cell death apparatus: EGL-1, CED9, CED4 and CED3 (Denton et al., 2013). CED3 is the homolog of mammalian caspases and is activated by the interaction with the adaptor protein CED4. This interaction occurs after the release of CED4 from the pro-survival protein CED9 (BCL-2-like), due to the sequestration of the latter by the BH3-only protein EGL-1 (Conradt and Horvitz, 1998; del Peso et al., 1998; del Peso et al., 2000; Yang et al., 1998). This core machinery is conserved in mammals, where one or more homologs of these proteins have been described. In mammalian cells two different pathways that lead to caspase activation have been identified: 1) in the extrinsic pathway, an extracellular death ligand (such as tumor necrosis factor-α, TNF-α) binds to a transmembrane "death-receptor" (Taylor et al., 2008). This interaction provokes the recruitment of adaptor proteins, such as FADD, which in turn recruit several Caspase-8 molecules. Caspase-8 is an initiator caspase that can autoactivate and cleave pro-Caspase-3 and pro-Caspase-7 (effector caspases); 2) in the intrinsic pathway, the apoptotic stimulus (cell stress or damage) is transduced to the mitochondria by BH3-only proteins, such as BID (Luo et al., 1998). This protein also mediates the cross-talk with the extrinsic pathway given that it can be targeted and cleaved by Caspase-8. If the activator effect of BH3-only proteins exceeds the inhibitory effect of anti-apoptotic BCL-2 family proteins, BAK-BAX oligomers assembly on the mitochondrial outer membrane, permitting the efflux of intermediate space proteins such as Cytochrome c (Jurgensmeier et al., 1998). Once released, it

promotes the assembly of the apoptosome, composed by several molecules of the apoptotic protease activating factor-1, APAF1, and Caspase-9 (Shiozaki et al., 2002). Caspase-9 propagates a proteolytic cascade that leads to the activation of the major effector caspases 3, 7 and 6, which possess proteolytic ability on several intracellular substrates, thus culminating in cell death (Taylor et al., 2008). In mammals, the activity of Caspase-3, 7 and 9 can be regulated also by IAPs (inhibitor of apoptosis proteins) (Riedl and Shi, 2004; Tenev et al., 2004). All the members of the caspase family share a similar structure consisting of a prodomain and a catalytic domain with peptidase activity. Initiator caspases usually possess a longer prodomain compared to effector caspases. The catalytic domain is composed by two subunits of about 10 and 20 kDa (Chang and Yang, 2000; Fuentes-Prior and Salvesen, 2004). After proteolityc cleavage of the proenzyme (zymogen), the two subunits form a heterodimer. The association of two heterodimers leads to the formation of the active caspase (Chang and Yang, 2000). Effector caspases orchestrate the dismantling of most of cell structures (Taylor et al., 2008). Proteolysis of the Rho effector ROCK1 determines the contraction of the actin cytoskeleton and plasma membrane blebbing, as well as nuclear fragmentation (Coleman et al., 2001). Cleavage of tubulins and microtubule-associated proteins contribute to the formation of apoptotic bodies (Moss et al., 2006). Caspase-mediated cleavage of nuclear lamins and envelope proteins leads to nuclear fragmentation (Rao et al., 1996). Proteolysis of MST1 protein results in its translocation to the nucleus, phosphorylation of Histone H2B and chromatin condensation (Cheung et al., 2003; Ura et al., 2001). Cleavage of Icad (inhibitor of caspase activated DNAse) determines inter-nucleosomal DNA cleavage (Enari et al., 1998). Caspase activity is

also required for the exposure of phosphatydilserine and other phagocytic signals on the cell surface (Martin et al., 1995).

1.4 Apoptosis in insects

The molecular pathway leading to caspase activation in insects has been mainly studied in *Drosophila melanogaster* and some differences, compared to *C. elegans* and mammals, have been underlined. Apoptosis in *D. melanogaster* involves effector caspases that are homologous to *C. elegans* CED-3, although the upstream pathway involves different proteins (Denton et al., 2013). In fact, in *Drosophila* homologs of EGL-1 are lacking and the two homologs of Bcl-2 identified so far play only minor roles in apoptosis (Chen and Abrams, 2000). In *Drosophila*, caspases are regulated mainly by IAP proteins that act through binding to central apoptotic players and whose removal is necessary for caspase activation (Deveraux and Reed, 1999; Hay et al., 1995). In this insect a precise distinction between intrinsic and extrinsic apoptotic pathway has not been described yet but orthologs of the TNF and TNF receptor family (Eiger and Wengen respectively) have been identified (Kauppila et al., 2003). Eiger can induce apoptosis and its effect is blocked by the IAP factor Diap1. Seven different caspases have been identified in *Drosophila*. Three of these are generally considered initiator caspases (Dronc, Dreed and Strica), based on the presence of a long prodomain, while the other four are classified as effector caspases (Drice, Dcp-1, Decay and Damm) (Denton et al., 2013). The initiator caspase Dronc can interact with the Ark/Dark molecule and assembly into an apoptosome similarly to what happens for mammalian Apaf-1 with Caspase-9 (Yu et al., 2006; Yuan et al., 2011). Dronc appears to be the essential initiator caspase in stress-induced and developmental apoptosis in this organism and Dronc null mutants

die during pupal stage, showing abnormalities in cell death pattern (Kumar and Doumanis, 2000; Daish et al., 2004). On the other hand, Dark does not require Cytochrome c for downstream caspase activation (Dorstyn et al., 2004). Dredd is related to mammalian Caspase-8 (Chen et al., 1998), but seems to be involved mainly in innate immunity. It is in fact activated by the Toll receptor and regulates the antimicrobial peptide expression pathway (Leulier et al., 2000; Stoven et al., 2003). The function of the *Drosophila* caspase Strica is still awaiting clarification and also its role as an initiator or as an effector caspase is a matter of debate. A redundancy between Strica and Dronc has also been proposed in some contexts (Baum et al., 2007; Denton et al., 2013). Concerning effector caspases, Drice is considered the functional analog of human Caspase-3 and is generally identified as the most relevant caspase in *D. melanogaster* (Kumar and Doumanis, 2000; Muro et al., 2006). On the other hand, Dcp-1 seems to play a minor and redundant role compared to Drice (Xu et al., 2006). Decay and Damm are the less studied caspases and their precise role has not been characterized yet (Denton et al., 2013).

The intervention of apoptosis during *Drosophila* development has been studied in different tissues. In *Drosophila*, 20E signaling stimulates apoptosis via EcR-USP and induces the expression of several apoptotic genes, including the caspases Dronc and Drice (Cakouros et al., 2004; Kilpatrick et al., 2005) and the death activators Reaper and Hid (Jiang et al., 2000; Lee et al., 2000). During metamorphosis apoptosis and autophagy are required for the correct degeneration of the salivary glands (Berry and Baehrecke, 2007). During abdominal muscle remodeling death occurs by apoptosis, and does not require autophagy (Zirin et al., 2013). On the other hand, despite high caspases levels were observed during midgut demise, apoptosis does not seem to play a

major role in this degenerative process (Denton et al., 2009). Apoptosis is also needed for the removal of the excess of nurse and follicle cells involved in oocyte maturation (Buszczak and Cooley, 2000). Caspase activity is also required during terminal differentiation of spermatids (Huh et al., 2004). In the same context, a Dronc-dependent but apoptosome-independent PCD has been described during the elimination of exceeding germ cells undergoing differentiation (Yacobi-Sharon et al., 2013).

In Lepidoptera, apoptosis and caspase activation are involved in the death of larval organs during metamorphosis, often in concomitance with autophagy. DNA fragmentation, apoptotic nuclei and caspase activation have been detected in several organs of different species of Lepidoptera during metamorphosis (Franzetti et al., 2012; Tettamanti et al., 2007; Therashima et al., 2000; Tian et al., 2012; Uwo et al., 2002). Active caspases and other apoptotic features have been also found, concurrently with autophagy, in the ovarian nurse cells of *B. mori* during oogenesis (Mpakou et al., 2006).

Similarly to *Drosophila*, 20E is one of the major regulators of apoptosis also in Lepidoptera (Tian et al., 2012). Manaboon et al. (2008) hypothesized that, in the anterior silk gland of *B. mori*, cell death is regulated by a double pulse of this hormone, which peaks twice during larval-pupal transition. The first peak of 20E (commitment peak) upregulates the expression of apoptosis-related genes and its effects are mediated by the EcR/USP receptor complex. The second pulse of hormone (metamorphic peak), which occurs during the pupal stage and is much stronger than the commitment peak, activates the so-called non-genomic response. This effect is mediated by a putative ecdysone membrane receptor and consists in the induction of effector caspases (Manaboon et al., 2008). Tian et al. (2012) showed that, in *B. mori* larval fat body, apoptosis and the expression of

apoptosis-related genes are induced by exogenous 20E and decreased by RNAi-mediated knockdown of USP. These results confirm that 20E induces apoptosis in the silkworm fat body during larval molting and larval-pupal transition.

Spodoptera frugiperda Caspase-1 was the first caspase identified and characterized in Lepidoptera (Ahmad et al., 1997). SfCaspase-1 is the main effector caspase in *S. frugiperda* and, during apoptosis, in Sf9 cells it is processed to mature subunits in a two-steps activation mechanism. The first step is the cleavage of the proenzyme (p37) at D^{195} (aspartic acid 195) residue thus producing p25 and the small subunit p12. The second step is the cleavage of p25 at D^{28} residue producing the large subunit p19 and the prodomain p6 (Lai et al., 2012; Liu and Chejanovsky, 2006) (Fig. 3).

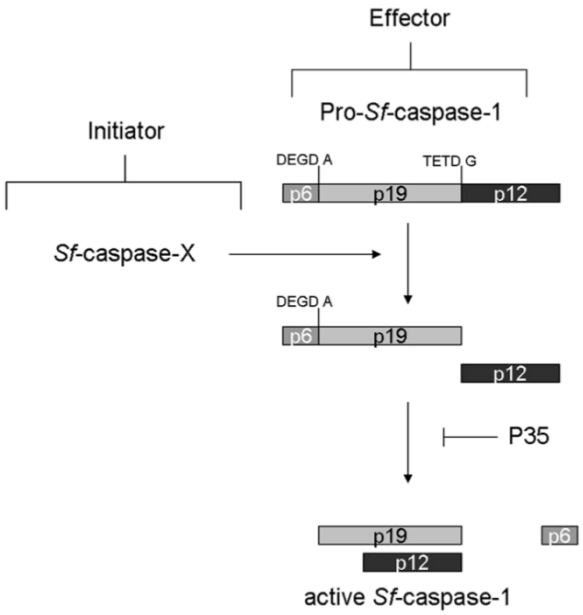

Figure 3 - Processing of lepidopteran pro-SfCaspase-1 into the active subunits (modified from Lai et al., 2012).

SfCaspase-1, SlCaspase-1 and BmCaspase-1 possess similar sequence and mechanism of action. Moreover, the three proteins contain the cleavage sites DEGD and TETD that are necessary for the processing of p19, p12 and p6 subunits (Liu et al., 2005).

In the study by Courtiade et al. (2011) caspases from several lepidopteran species were characterized, classified and compared to *Drosophila* homologs. Nucleotide sequences from 27 different lepidopteran species (including *B. mori*) were analyzed. Several putative caspases were identified and classified into six subgroups (from Caspase-1 to Caspase-6). Lepidopteran Caspase-1, 2 and 3 were considered effector caspases based on the structure of the prodomain and thus homologs to *Drosophila* Dcp-1, Drice and Decay. It is important to underline that in *B. mori* only two effector caspases have been found (Caspase-1 and Caspase-3) because of the lack of Caspase-2 homologs. Lepidopteran Caspase-5 and 6 show structural features typical of initiator caspases and share similarities with *D. melanogaster* Dronc and Dreed, respectively. Conversely, the function of Caspase-4 as an effector or an initiator caspase remains uncertain and functional studies are required to obtain more information about this issue (Courtiade et al., 2011). These results partially overlap those reported in a different study performed in *B. mori.* In that case, two initiator caspases, named BmDronc and BmDreed, and three effector caspases, BmCaspase-N, BmCaspase-1 and BmICE, were identified (Zhang et al., 2010). Moreover, a number of homologs of both human and *Drosophila* apoptosis-related genes, were reported and the presence of both the extrinsic and the intrinsic apoptotic pathway was hypothesized (Zhang et al., 2010). Even though the information on the apoptotic pathway in Lepidoptera is growing, it is still fragmentary compared to other model organisms such as *Drosophila* or mammals (Courtiade et al., 2011) (Fig. 4).

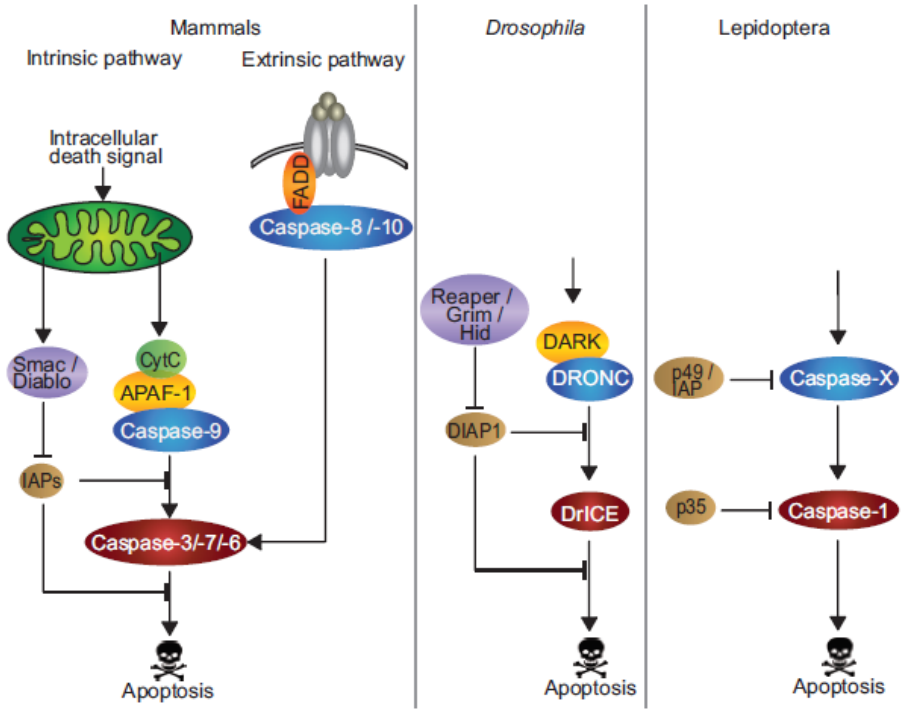

Figure 4 – Comparison between the apoptotic pathway in mammals, *Drosophila* and Lepidoptera (modified from Courtiade et al., 2011).

1.5 Autophagy

Autophagy is widespread in eukaryotes (Reggiori and Klionsky, 2002). Three different types of autophagy have been described so far:

- Chaperone Mediated Autophagy (CMA) can selectively target soluble cytosolic proteins that show the "KFERQ" aminoacid sequence. These proteins are recognized by cytoplasmic chaperones and translocated across the lysosomal membrane in a process mediated by membrane receptors (Dice, 1990). CMA is activated in response to starvation, oxidative stress, or toxic compounds (Bejarano and Cuervo, 2010);
- Microautophagy is a non-selective process of degradation of intracellular components that involves direct engulfment of the

cytoplasmic cargo by invagination of the lysosomal membrane. Microautophagy can be induced by nitrogen starvation or rapamycin and is involved in the maintenance of organelle size, membrane homeostasis, and cell survival under nitrogen restriction (Li et al., 2012; Wang and Klionsky, 2004);

- Macroautophagy, hereafter termed autophagy, is the most common and, by far, the better studied among these processes. It can be described as the sequestration of portions of cytoplasm and organelles within autophagosomes and the subsequent cargo degradation following authophagosome-lysosome fusion. It is believed that autophagy is involved in a great variety of physiological and patho-physiological processes such as response to starvation, clearance and turnover of proteins and organelles, development, aging, immune response, cell death, and tumor suppression (Mizushima, 2005).

The autophagic process starts with the formation of an isolation membrane or phagophore. The assembly point of the phagophore is called preautophagosomal structure or Phagophore Assembly Site (PAS). The source of the membrane used to build up the autophagosome has been matter of debate for a long time. The first hypothesis, based on morphological and immunohistochemical analysis, pointed out that the ER, Golgi or *de novo* synthesis were the most likely source of this membrane (Tooze and Yoshimori, 2010). *De novo* synthesis was originally supported by the observation that the autophagosomal membrane is poor in protein content and free from known organelle markers. Recent discoveries have shown that the ER (Hayashi-nishino et al., 2009; Yla-anttila et al., 2009) and the mitochondria (Hailey et al., 2010) could be a likely source of membrane. Furthermore, Hamasaky et al. (2013) postulated that autophagosomes form at ER-mitochondria contact sites. Due to the peculiar mechanism of formation, autophagosomes are surrounded by a double-

membrane. This feature allows to distinguish them from other vesicles such as endosomes, lysosomes or apoptotic blebs by transmission electron microscopy (TEM). The fusion between autophagosomes and lysosomes generates autolysosomes. In autolysosomes the autophagosome inner membrane and its cargo are degraded by lysosomal hydrolases (Kroemer et al., 2009). The entire autophagic process, which comprises autophagosome formation, maturation, fusion with lysosomes, breakdown and release of molecules into the cytoplasm, is usually termed "autophagic flux" (Zhang et al., 2013) (Fig. 5).

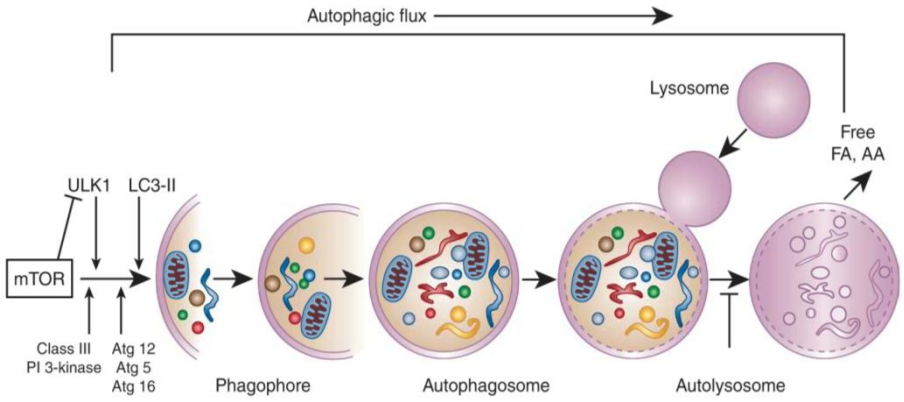

Figure 5 - Representation of the autophagic flux (adapted from Kaushal et al., 2012).

More than thirty autophagy-related (Atg) proteins were described in yeast and about twenty in mammals. In fact, autophagy involves the coordinated activation of multiple molecular components. Atg proteins can be classified into six functional groups: the Atg1/Ulk1 kinase complex, Atg9, the Class III PI3K (Vps34 - Beclin1) complex, the PI(3)P-binding Atg2-Atg18 complex, the Atg12 and the Atg8 ubiquitin-like conjugation systems (Itakura and Mizushima, 2010).

Atg1 (Ulk1 in mammals) is an evolutionary conserved serine/threonine protein kinase that associates with other proteins (including Atg13, Atg101 and FIP200), thus forming a complex. The activation of the Atg1 complex is considered the most upstream step in autophagosome formation (Suzuki et al., 2007). Atg1/Ulk1 has at least two distinct roles in the activation of autophagy: it mediates the recruitment of Atg proteins and also plays a role in the subsequent formation of autophagosomes in both yeast and mammalian cells (Mizushima, 2010). There are several Atg1 homologs in mammals named Ulk2, Ulk3, Ulk4 and Stk36 with less clear roles compared to Ulk1. Studies conducted in *Drosophila* and mammals identified a direct interaction between Atg1/Ulk1 complex and the protein kinase Tor (Target Of Rapamycin) (Chang and Neufeld, 2009; Nazio et al., 2013). Tor is a master regulator of the nutrient signaling pathway and a negative regulator of autophagy. Tor acts downstream of growth factor receptor signaling, hypoxia, ATP levels and insulin signaling. Moreover, the chemical rapamycin inhibits the activity of Tor, thus promoting the formation of the Atg1/Ulk1 complex. Furthermore, in *Drosophila* and other insects Tor pathway activity is decreased by 20E (Rusten et al., 2004; Tian et al., 2013). Tor associates with other proteins thus forming the complex Torc1, which was demonstrated to regulate the autophagic response. Moreover, the level of Tor phosphorylation is directly linked to the activity of this complex. The activity of Atg1 complex on phagophore formation is mediated by the transmembrane protein Atg9, which probably acts by promoting lipids recruitment to the isolation membrane (Glick et al., 2010). Accordingly, it was demonstrated that Atg1 phosphorylates Atg9 during the early steps of autophagy activation in yeast (Papinsky et al., 2014). The nucleation of the isolation membrane is activated by the Vps34-Atg6/Beclin-1 complex. Vps34 is a class III PI3K able to generate PI3P, which is essential

for phagophore elongation and recruitment of other Atg proteins to the assembly site. The catalytic activity of Vps34 is promoted by its interaction with Beclin-1 and leads to an increase in the PI3P levels. This complex is inactivated by anti-apoptotic proteins that belong to the Bcl-2 family and by other signaling molecules (Mariño et al., 2014; Pattingre et al., 2005). Class III PI3K inhibitors, such as 3-methyladenine and wortmannin, block the production of PI3P and are among the most commonly used autophagy inhibitors (Wu et al., 2010). Once autophagy is activated, two ubiquitin-like systems allow the extension of the phagophore and the formation of the autophagosome. The first ubiquitin-like system mediates the conjugation of Atg12 with Atg5. In the first step of this process Atg7 activates Atg12. Atg10 then mediates the conjugation of activated Atg12 with Atg5 (Glick et al., 2010). Atg5-Atg12 forms a complex with Atg16L which binds to the extending phagophore. This association induces the curvature of the growing membrane through the asymmetric recruitment of processed Atg8-PE (LC3-II in mammals) (Glick et al., 2010). The second ubiquitin-like systems allows the processing of Atg8/LC3. Whereas yeast has a single Atg8 gene, multicellular animals have several. Atg8 proteins comprise three subfamilies: microtubule-associated protein 1 light chain 3 (MAP1LC3 or LC3), γ-aminobutyric acid receptor-associated protein (GABARAP) and Golgi-associated ATPase enhancer of 16 kDa (GATE-16). Humans possess a single GATE-16, two GABARAP, and four LC3 proteins (Shpilka et al., 2011). LC3 is expressed as a full-length cytosolic protein and is cleaved by the cysteine protease Atg4 to generate LC3-I (Kirisako et al., 2000). LC3-I is activated by Atg7 (in a fashion similar to Atg12), transferred to Atg3 and conjugated to phosphatidylethanolamine (PE), to generate LC3-II/Atg8-PE (Ichimura et al., 2000). LC3-II/Atg8-PE is found on both sides of the autophagosome membrane (Kabeya et al., 2000). In mammals

LC3-related molecules can undergo similar processing and co-localize with LC3-II on the autophagosome. Even though the precise role of these molecules is still not clear, it is probably related to cargo selection by the autophagosome (Shpilka et al., 2011) and autophagosome biogenesis (Kabeya et al., 2004). Autophagy was initially regarded as a non-selective process of degradation because electron micrographs frequently show autophagosomes containing mixed cytoplasmic components (Eskelinen, 2008). On the other hand, emerging evidence pointed out that phagophore membrane can selectively interact with cytoplasmic protein aggregates and organelles. It was proposed that LC3-II plays a role in the autophagosomal cargo selection, acting as a receptor that interacts with adaptor molecules on the target. In this context, the most studied adaptor protein is p62/SQSTM1. This molecule promotes the turnover of proteins tagged with Lys63-linked ubiquitin chains. p62 interacts with poly-ubiquitinated proteins via its ubiquitin binding domain (UBD), and with LC3-II through its LC3-interacting region (LIR). Other proteins such as Nbr1 seem to have a role similar to p62 (Johansen and Lamark, 2011). Moreover, it was proposed that Uth1p and Atg32 promote selective mitophagy in yeast (Kanki et al., 2009; Kissova et al., 2004). Once formed, autophagosomes fuse with lysosomes, thus forming autolysosomes. The fusion is mediated by several SNARE-like proteins that are localized both on autophagosomes and lysosomes (Liu R et al., 2015). This process involves the action of the cytoskeleton and needs the presence of the proteins LAMP-1 e LAMP-2 on the lysosomal surface (Eskelinen, 2006).

Several assays have been developed to assess the activation of autophagy in a specific context. For a comprehensive review of the methodologies used for this purpose refer to the "Guidelines for the use and interpretation of assays for monitoring autophagy" (Klionsky et al., 2012). From a morphological point of view the

hallmarks of autophagy can be defined as the presence of phagophore sequestering portions of cytosol and the presence of autophagosomes that can be distinguished from other cytoplasmatic compartments due to the presence of the double membrane. TEM can be used for both qualitative and quantitative analysis in the field of autophagic research (Klionsky et al., 2012). Although this methodology is one of the most used to monitor autophagy, it is also subjected to misinterpretations mostly deriving from methodological artifacts. The main issues, when using TEM, are related to the precise identification and distinction of autophagic compartments and contents. These problems can be partially solved through immuno-TEM approaches, by using antibodies that are able to recognize autophagosomal or cargo antigens (Eskelinen et al., 2011; Klionsky et al., 2012).

Another widely used method for the assessment of the activation of the autophagic flux is the quantification of the Atg8-PE/LC3-II protein by immunoblotting or by using GFP-LC3/Atg8 expressing cells. The measurement of the protein levels or the number of LC3-II/Atg8-PE dots, is considered an affordable marker of the amount of autophagosomes in the cell (Klionsky et al., 2012). In addition to LC3, other proteins involved in autophagy, such as SQSTM1/p62, Atg1/Ulk1 or Atg6/Beclin-1, can be used as autophagic markers. The level of activation of Torc1, indirectly monitored by measuring the phosphorylation of specific downstream targets (e.g., EIF4EBP1), can also be used to gain information regarding autophagy. One major issue while using autophagy markers is that the autophagic flux is a dynamic process composed of several steps that can be modulated at different points. For instance, an accumulation of autophagosomes can reflect induction of autophagy, reduction in autophagosome turnover or the inability of turnover after an increase in autophagosome formation (Klionsky et al., 2012). Thus, caution

must be used when trying to assess the level of activation of autophagy. Moreover, the concurrent use of more than one marker is highly recommended. In some settings, such as development-related processes in *Drosophila*, also the expression of *ATG* genes has been used to obtain indirect information on the activation of autophagy. Other indirect autophagy assays, such as the measurement of acid phosphatase activity or the staining with acidotropic dyes, are useful to evaluate the activation of the lysosome pathway, which usually occurs concomitantly with the activation of autophagy (Klionsky et al., 2012).

1.6 Developmental programmed autophagy in insects

The molecular bases of autophagy have been thoroughly investigated in the recent past, evidencing a deep conservation among metazoans. This justifies the use of arthropod models to obtain information on the role of autophagy in more complex organisms (Malagoli et al., 2010). In particular, the demise of larval organs in holometabolous insects during metamorphosis represents an ideal model to study the role of autophagy in degenerative settings and in relation to apoptosis (Franzetti et al., 2012).

It was demonstrated that, in *Drosophila*, autophagy actively intervenes together with apoptosis during the metamorphic removal of salivary glands. Incomplete degradation of this organ is observed after *ATG* genes knockout or knockdown. Furthermore, overexpression of *ATG1* induces the premature degradation of salivary glands without any involvement of caspases (Berry and Baerecke, 2007). Autophagy is also necessary for larval midgut degeneration. Similarly to salivary glands, loss-of-function *ATG* mutants or knockdown of *ATG1* and *ATG18* severely impairs midgut removal. In addition, the high level of caspases detected in this context seems to be dispensable for midgut degeneration

(Denton et al., 2009). In the fat body, *ATG1* overexpression is sufficient to induce caspase-dependent cell death where degenerating adipocytes show apoptotic features, thus corroborating the hypothesis that autophagy can induce apoptosis (Scott et al., 2007). Autophagy and components of the apoptotic machinery are also required during *Drosophila* oogenesis. In this setting, the removal of the IAP dBruce mediated by autophagy is required to induce caspase activation and occurrence of apoptosis (Nezis et al., 2010).

In Lepidoptera, homologs of several components of the autophagic pathway have been identified. These include multiple *ATG* genes and other genes involved in the PI3K signal transduction pathway (Zhang et al., 2009). A comprehensive list of references reporting the analysis of *ATG* genes and proteins in Lepidoptera can be found in Romanelli et al. (2014). Autophagic features have been frequently observed in many lepidopteran organs that die during metamorphosis, such as the *Heliothis virescens* midgut (Tettamanti et al., 2007), the *M. sexta* fat body (Muller et al., 2004) and the fat body (Tian et al., 2013), the silk gland (Li et al., 2010) and the midgut (Franzetti et al., 2012) of *B. mori.* In the silkworm midgut, autophagy is activated at wandering stage, when a large number of autophagic compartments, an increase in acid phosphatase activity and BmAtg8 processing to BmAtg8-PE can be detected (Franzetti et al., 2012). In this context autophagy is set in motion once the larva stops feeding to cope with starvation, leading to a reduction of the total protein concentration and inducing an increase in ATP levels.

Tian and colleagues (2013) demonstrated that in the fat body of *B. mori* autophagy is activated simultaneously with the 20E commitment peak during larval-pupal transition. Accordingly, 20E injection in *B. mori* larvae leads to *ATG* genes upregulation, Torc1 inhibition and Atg8 processing to Atg8-PE. Moreover, autophagy is

reduced by RNAi of *ATG1* and *USP* genes and *EcR* dominant-negative mutants show reduced autophagic induction during metamorphosis. These results clearly show that 20E is able to increase autophagy by inhibiting the PI3K/Torc1 pathway, allowing the activation of the downstream Atg1/Atg13 complex. 20E is also able to stimulate autophagosome formation by acting on the receptor complex EcR/USP that, in turn, activates the transcription of *ATG* genes. The authors also demonstrated that *ATG* genes can be activated both directly (this happens for *ATG1* thanks to the presence of an ecdysone response element in the promoter) and indirectly (through the action of Br-C and downstream proteins). In conclusion, it has been proposed that in this setting autophagy functions to exploit nutrients from the adipose tissue in order to support the growth and differentiation of the adult structures (Tian et al., 2013). This working model is in accordance with that reported for *Drosophila* fat body, where inhibition of the PI3K/Tor signaling by 20E activates autophagy (Rusten et al., 2004). As already mentioned for *Drosophila,* in *B. mori* feeding larvae autophagy can also be stimulated by injecting rapamycin. However, the effect elicited in the silkworm fat body is weaker than that observed following the treatment with 20E, probably reflecting the inability of rapamycin to increase the expression levels of all the key *ATG* genes (Tian et al., 2013).

In addition to 20E, also JH seems to be involved in the regulation of autophagy in insects. The common view is that JH inhibits autophagy befoure metamorphosis. Accordingly, it has been demonstrated that the treatment of *Mamestra brassicae* with JH during the last larval instar inhibits autophagy in the fat body (Sass and Kovacs, 1975). This result suggests that autophagy is activated when 20E concentration increases, provided that JH titer is low. In Lepidoptera, there is limited information on the signaling pathway that links JH to autophagy. However, it has been reported

that RNAi of the putative JH receptor Met in *B. mori* has a marked effect on the autophagic response during metamorphosis (Guo et al., 2012).

As in other organisms, also in Lepidoptera Atg8 processing to Atg8-PE is considered the most reliable marker to assess the activation of autophagy. One peculiarity of lepidopteran Atg8 (as well as *Drosophila* Atg8a and Atg8b), that must be kept in mind when using this autophagic marker, is that it belongs to GABARAP protein family instead of MAP1LC3 family (Hu at al., 2010). The measure of Atg8-PE level as a marker of autophagy has been used in Lepidoptera in different settings: during development (Franzetti et al., 2012; Khoa and Takeda, 2012; Tian et al., 2013), under starvation conditions (Khoa and Takeda, 2012) and in lepidopteran cell lines (Gai et al., 2013). TEM analysis, *ATG* gene expression, acid phosphatase and acidotropic dyes have been also used as markers of autophagy in these contexts (Franzetti et al., 2012; Tian et al., 2013).

1.7 The interplay between autophagy and apoptosis

A coexistence of autophagy and apoptosis has been described in several biological settings but the role and the relationship between these two processes is usually context-specific. In general, two main functions have been proposed: autophagy can have a pro-survival role, thus inhibiting apoptosis, or it can directly (autophagic cell death) or indirectly (via the activation of apoptosis) lead to the demise of the cell (Eisenberg and Lerner, 2009; Mariño et al., 2014).

Different types of stress can induce both autophagy and apoptosis. In the case of a pro-survival role of autophagy, this process usually precedes apoptosis and is activated until the level of the stimulus is relatively low. On the contrary, apoptosis intervenes

when the duration or the intensity of the stress exceeds a critical threshold. In this case autophagy is needed by the cell to adapt to the stimulus. For example, this happens after the exposition to external factors such as scarcity of essential nutrients (starvation), inhibition of growth factor receptors or administration of ionizing radiations and chemotherapics. Intercellular signals such as the level or localization of p53, BH3-only proteins and JNK are other stimuli which regulate both autophagy and apoptosis in the same fashion (Pattingre et al., 2005; Tasdemir et al., 2008; Wei et al., 2008). There are many ways in which autophagy can prevent apoptosis: in some settings, the selective autophagic degradation of mitochondria (mitophagy) can increase the resistance of the cells to a lethal stimulus. In fact, damaged mitochondria can be selectively directed to autophagosomes, thus preventing mitochondrial outer membrane permeabilization and the activation of the intrinsic apoptotic program (Youle and Narendra, 2011). Autophagy can also be responsible for the selective reduction of the levels of pro-apoptotic proteins in the cytosol, thereby preventing the onset of apoptosis. Once apoptosis is activated, pro-survival autophagy is inhibited by the caspase-mediated cleavage of essential components of the autophagy pathway, such as Atg3 (Oral et al., 2012) or Beclin1 (Wirawan et al., 2010).

On the contrary, autophagy or essential autophagic proteins can promote cell demise. In these cases inhibition of autophagy prevents cell death. For instance, it has been proposed that Caspase-8 requires the presence of the autophagosomal membrane as a platform for its processing, and knockout of *ATG* genes reduces the activation of both Caspase-3 and 8 (Young et al., 2012). In *Drosophila*, where apoptosis is regulated mainly by IAPs, autophagy is able to degrade the protein dBruce thus activating apoptosis (Nezis et al., 2010). Moreover, developmental apoptosis is prevented by mutations of Atg1, Atg13 or Vps34 and

stimulated by the overexpression of Atg1 (Scott et al., 2007). Atg proteins can also contribute to lethal signaling independently from the activation of autophagy. One of the most significant examples is the calpain-mediated cleavage, and the subsequent translocation from the cytosol to the mitochondria, of Atg5. The cleaved protein can then associate with the anti-apoptotic molecule Bcl-xL to trigger Cytochrome c release and caspase activation (Yousefy et al., 2006). Other examples of Atg proteins involved in apoptosis induction are Atg12, which depletion reduces caspase activation, and Atg7, that can facilitate the onset of apoptosis in specific contexts (Kessel et al., 2012; Rubinstein et al., 2011).

These scenarios have been postulated mainly based on studies performed in yeast, mammals and *Drosophila,* but the coexistence of autophagic and apoptotic features has been frequently described in Lepidoptera as well (Franzetti et al., 2012; Tettamanti et al., 2007; Tian et al., 2012; Tian et al., 2013). It is likely that this copresence is due to an overlap in their regulatory pathways also in these organisms (Romanelli et al., 2014). In fact, it has already been demonstrated that 20E mediates the developmental activation of both autophagy and apoptosis in Lepidoptera, too (Matsui et al., 2012; Sekimoto et al., 2006; Tian et al., 2012; Tian et al., 2013). Moreover, it has been proposed that the induction of apoptosis after 20E- or starvation-induced autophagy can be mediated by BmAtg5 and BmAtg6 in *B. mori* cell lines (Sheng Li, personal communication).

1.8 The silkworm, Bombyx mori

The experimental model used in this study is the lepidopteron *B. mori,* or mulberry silkworm. *B. mori* is considered the only truly domesticated insect that is completely dependent on humans for

its growth and reproduction (Goldsmith et al., 2005). The silkworm plays key roles in several fields: basic research, insect biotechnology and sericulture (Goldsmith et al., 2005). Among insects, its importance as a model for genetic studies is second only to *Drosophila*, due to the availability of numerous genetic and molecular biology tools, such as gene transfer, RNAi-mediated silencing, and a completely sequenced genome (Wang et al., 2005). Moreover, it is one of the most valuable models for research on Lepidoptera because of the indisputable advantages due to the large number of information gathered on its developmental biology, physiology and endocrinology (Xia et al., 2014). As a lepidopteran model organism *B. mori* can also be useful in the field of insect pest management. In fact, many Lepidoptera are pest insects that cause massive damages to economically valuable crops. The widespread use of broad spectrum pesticides has progressively led to pesticide resistant insects, a reduction in beneficial insect populations and harmful effects to humans and the environment. Thus, in last years, research has been trying to develop environmentally friendly strategies for the control of pests (Stevens et al., 2012). Lastly, as the natural source of silk, *B. mori* is also important for the sericulture industry. In fact, silk is still considered one of the most valuable materials for textile industries. Moreover, it has recently gained attention as a biomaterial with several desirable properties. In particular, these include biocompatibility, the possibility of being chemically modified, the slow rate of degradation *in vivo*, and the ability to be processed into different forms (Reddy and Prasad, 2011).

1.9 The life cycle of B. mori

B. mori is a holometabolous insect with a life cycle composed of four stages: egg, larva, pupa and adult. After the egg hatches, the larva goes through five larval instars separated by molts. The larva spends much of the time feeding on mulberry leaves (or artificial diets) and grows quickly. At the end of the fifth larval instar the caterpillar stops feeding and spins a cocoon that protects the larva during metamorphosis. The larva metamorphoses to pupa, and then to adult, in about ten days and then emerges from the cocoon (Fig. 6).

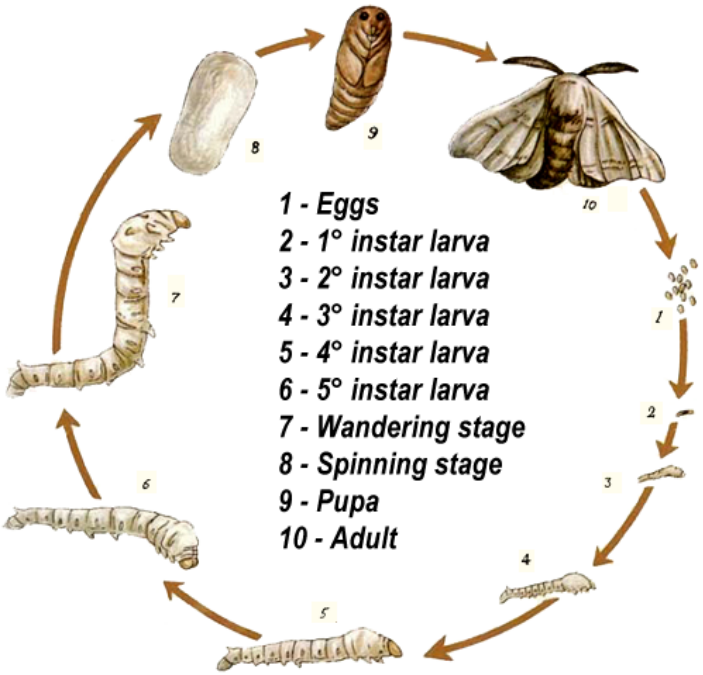

Figure 6 - Life cycle *of B. mori*.

The whole process from hatching to adult eclosion lasts about 36 days at 25 °C. The adult does not feed and spends much of the time mating. The fecundated eggs are laid and need specific

artificial treatments to hatch in laboratory condition (Tazima, 1978).

1.10 The silkworm midgut

In lepidopteran larvae, the alimentary canal has a simple structure constituted of three regions named the foregut, the midgut and the hindgut. The foregut is the most anterior part, represents a vestigial apparatus and is very short (Dow, 1986). The hindgut is subdivided in an anterior region called ileum, where the excess of fluid in the digested material is squeezed, and in a posterior part or rectum, from where the undigested materials pass out through the anus (Dow, 1986). The larval midgut represents the middle and, by far, the most extended region of the digestive tract, which carries out digestive and absorptive functions, and occupies most of the body cavity (Dow, 1986). This organ is lined by the peritrophic matrix that represents a selective barrier to the passage of molecules and protects the epithelium from mechanical damage, bacterial infection and toxins (Terra, 2001). The larval midgut is composed by a monolayered epithelium supported by a basal lamina, striated muscles and tracheoles. Four cell types can be distinguished in the midgut epithelium according to morphological and functional features. Columnar and goblet cells, which are the main cell types, are involved in the uptake and secretion activity, respectively (Dow, 1986). A brush-border, that facilitates nutrient absorption, is present on the apical membrane of columnar cells. Goblet cells show a large intracellular cavity that communicates with the lumen via an apical valve. Sparse stem cells, which are able to differentiate into mature columnar and goblet cells, are localized at the base of the epithelium (Baldwin et al., 1996; Hakim et al., 2010). Stem cells take part to the growth of the epithelium during larval-larval moults, the generation of the

adult midgut during metamorphosis and the regeneration of tissues in case of damage (Franzetti et al., 2015; Hakim et al., 2010; Tettamanti et al., 2007). Furthermore, few and scattered endocrine cells, which secrete hormones, are present in the basal region of the epithelium (Endo and Nishiitsutsuji-Uwo, 1981). These cells play a role in the differentiation of stem cells and in the secretion of digestive enzymes (Wigglesworth, 1972).

At the end of the fifth instar the larva enters the so-called wandering stage, which precedes the spinning of the cocoon. At this stage the larva stops feeding and gut purging occurs. During the spinning and prepupal phase, the midgut becomes progressively shorter and folds are visible on the outer surface. During pupal stage, the morphological modification of this organ continues and, after adult eclosion, a conical midgut is observed. Light microscopy observations revealed that these changes in the midgut appearance were accompanied by degeneration and regeneration events in the midgut tissues (Franzetti et al., 2012). In fact, during the wandering and spinning stage a new midgut epithelium (pupal-adult midgut) is formed by the proliferation and differentiation of stem cells. Concomitantly, the larval midgut is pushed towards the lumen by the newly forming epithelium and starts to degenerate: cells modify their morphology, lose their reciprocal contacts, give rise to a compact mass of cells (named yellow body), that progressively disappears. During the degeneration of larval midgut cells morphological and molecular features of both autophagy and apoptosis have been observed. On the other hand, the precise role of the two processes, as well as a possible interaction between them, has not been demonstrated in this setting. In a recent study, it has been hypothesized that autophagy is needed to gain nutrients and recycle materials derived from epithelial cells before the onset of apoptosis. These

molecules can be absorbed by the new adult epithelium (Franzetti et al., 2015) (Fig. 7).

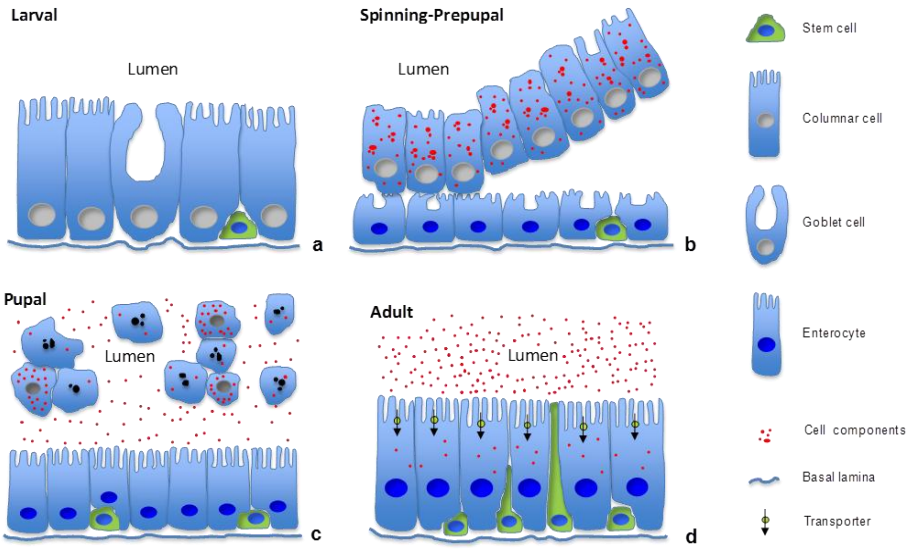

Figure 7 - Model proposed for the remodeling of the midgut during metamorphosis (adapted from Franzetti et al., 2015).

1.11 Aim of the work

The present study has three main aims:

- the molecular characterization of PCD-related processes involved in the developmental demise of the larval midgut in *B. mori*;
- the characterization of the regulatory pathways of autophagy and apoptosis in this setting;
- the analysis of the role of apoptosis and autophagy, and their relationship, in the degeneration of the silkworm midgut.

2 MATERIALS AND METHODS

2.1 Experimental animals

Larvae of a *B. mori* four-way polyhybrid strain (126x57)(70x90) were provided by CRA Honey Bee and Silkworm Research Unit (Padova, Italy). The larvae were fed on artificial diet (Cappellozza et al., 2005) and reared at 25 ± 0.5 °C under a 12:12 hours light:dark period and 70% relative humidity. After animals had ecdysed to the last larval instar, they were staged and synchronized according to the morphological features listed in Table 1.

Stage	Definition	Larval Features	Midgut description
L5D1-L5D6	Fifth larval instar day 1–day 6	The larva actively feeds	The larval midgut epithelium is well-organized
W	Wandering stage	The larva stops feeding; spinneret pigmentation and gut purging occurs	The larval midgut epithelium is well-organized; stem cells start to proliferate
SD1	Spinning stage day 1	The larva starts spinning the cocoon	The larval midgut epithelium starts to degenerate; stem cells proliferate
SD2	Spinning stage day 2	Cocoon spinning is completed	The larval midgut epithelium detaches from the pupal epithelium; active formation of the new pupal epithelium
PP	Prepupal stage	The metamorphosis from larva to pupa occurs	The larval midgut epithelium is shed into the lumen (yellow body); the new pupal epithelium continues to grow and differentiate
P1-P9	Pupal stage day 1–day 9	Pupa	Yellow body is actively degraded; the new pupal epithelium differentiates into the adult midgut

Table 1 - Definition and description of developmental stages of the silkworm, *B. mori*, used in this study.

Silkworms at the desired stage were quickly anesthetized with CO_2. Midgut dissection was performed by using a SZ30 Stereomicroscope (Olympus, Tokio, Japan).

2.2 Functional experiments

In order to analyze the role and regulation of autophagy and apoptosis, larvae were treated with different chemicals during the feeding or spinning stage: 20E (Sigma, St. Louis, USA), rapamicyn (Sigma), z.vad.fmk (Promega, Fitchburg, USA), and chloroquine (Sigma). For more information on the amounts and the timing of each treatment in different experiments, refer to the "Results" section. Injections were performed in one of the prolegs (first pair) in order to avoid the damage of internal organs, by using a Hamilton 701N syringe (Hamilton, Reno, Nevada). The proleg was disinfected with 70% ethanol before and after the injection. Larvae were kept under observation for some minutes after the treatment to avoid possible leaks of hemolymph. Control larvae were injected with an equal amount of solvent. Larvae were collected 6, 24, 48 and/or 72 hours after the treatment for morphological examination and molecular biology analyses (see "Results" for more information).

2.3 Quantitative real-time PCR (qRT-PCR)

Midguts were dissected, cleaned from residues of fat body and tracheae and immediately frozen in liquid nitrogen until use. Total RNA was isolated from 20-40 mg of frozen tissue using Trizol Reagent (Life Technologies, Carlsbad, USA) according to manufacturer's instructions with only slight modifications. RNA was treated with TURBO DNA-free Kit (Life technologies) to remove possible genomic DNA contaminations and integrity was assessed

by electrophoresis. RNA was retrotranscribed to cDNA using M-MLV reverse transcriptase (Life Technologies). Primers used for qRT-PCR are listed in Table 2.

Gene	Genbank number	Primer sequences
BmATG1	NM_001309546.1	F: CCCCGCCTATGTCTATGTTG R: ATCTGATGGGTGGGAGTACG
BmATG8	NM_001046779.1	F: CCAGATCGCGTTCCTGTAAT R: GAGACCCCATTGTTGCAGAT
BmCASPASE-1	NM_001043585	F: GCCTGTCGAAAGATACGCTC R: CACAGCAACCAGCAGACAAT
BmCASPASE-5	NM_001195467.1	F: TCGCCATCCCGTGCTTTC R: GTTGACCCCGTCCCTGTTG
BmRP49	NM_001098282.1	F: AGGCATCAATCGGATCGCTATG R: TTGTGAACTAGGACCTTACGGAATC

Table 2 - Accession number and primer sequences used for the amplification of apoptosis- and autophagy-related genes.

qRT-PCR was performed using the iTaq Universal SYBR Green Supermix (Biorad, Hercules, USA) and a 96-well CFX Connect Real-Time PCR Detection System (Biorad). $2^{-\Delta\Delta Ct}$ method, with *BmRP49* as a housekeeping gene, was used to calculate the relative expression of the genes of interest. Efficiency of the reaction amplification for each couple of primers was tested and adjusted to be in the range of 90-105%. *BmRP49* was reported to be stable across developmental stages in *B. mori* (Teng et al., 2012) and used in previous studies on silkworm metamorphosis (Tian et al., 2012; Tian et al., 2013). Each value was the result of experiments performed on midguts isolated from 3 to 8 series of animals. Statistical analysis was performed using Student's T-Test or Anova followed by Tukey HSD test.

2.4 Evaluation of anti-Gabarap antibody

BmAtg8 recombinant protein was expressed in BL21DE3/pET28+BmAtg8 bacteria (Franzetti et al., 2012). pET28+BmAtg8 expression vector was provided by Prof. Congzhao Zhou (University of Science and Technology of China). The anti-HsGabarap antibody (Abcam, Cambridge, UK) was tested against BmAtg8 recombinant protein and silkworm tissue protein extracts by immunoblotting.

2.5 Western blot analysis

Midgut dissection and storage was performed as described above for qRT-PCR samples. For western blot analysis, total proteins were extracted as follows. 20-60 mg of midgut tissue was homogenized with a T10 basic ULTRA-TURRAX (IKA, Staufen, Germany) in 10 µl/mg tissue of RIPA buffer (150 mM NaCl, 2% NP-40, 0.5% sodium deoxycholate, 0.1% SDS, 50 mM Tris pH 8.0), freshly added with 1X protease inhibitor cocktail (Thermo Fisher Scientific, Waltham, USA) and phosphatase inhibitors (1mM sodium orthovanadate, 5mM sodium fluoride). Homogenates were clarified by centrifugation (15000 × g for 15 min at 4 °C). Proteins were mixed with 2X gel loading buffer and denatured by heating the samples at 98 °C for 5 min. SDS-PAGE was performed on a 12% tris-glicine or 10% tris-tricine acrylamide gel by loading 40 µg protein per lane. After electrophoresis, the proteins were transferred to 0.45 µm nitrocellulose (Thermo Fisher Scientific) or 0.45 µm PVDF membranes (Merck Millipore, Billerica, USA). Membranes were saturated with a solution of 5% milk for 1 hour at room temperature and subsequently incubated with primary antibodies anti-Gabarap diluted 1:2500, anti-p4EBP1 (Cell Signalling, Danvers, USA) diluted 1:1000, anti-Caspase-3 (Cell

Signalling) diluted 1:1000, anti-Cleaved Caspase-3 (Cell Signalling) diluted 1:1000 for 2 hours at room temperature. Antigens were revealed with an appropriate HRP-conjugated secondary antibody (Jackson Immuno Research Laboratory, West Grove, USA) diluted 1:7500 (anti-rabbit) or 1:5000 (anti-mouse). Immunoreactivity was detected with SuperSignal West Pico Substrate (Thermo Fisher Scientific). Anti-Gapdh (Proteintech, Chicago, USA) diluted 1:2500 or anti-Tubulin (Sigma) diluted 1:10000 antibodies were used for housekeeping proteins detection. Since the use of "housekeeping proteins'" as internal standards was unsuitable when comparing different developmental stages (Franzetti et al., 2012), we adopted a Coomassie staining procedure (Welinder et al., 2011) to assess equal gel loading and blotting efficiency.

2.6 Immunofluorescence

Midguts were excised from the animal and fixed in 4% paraformaldehyde in 0.1 M phosphate-buffered saline (PBS, pH 7.2) for 3 hours at room temperature. Specimens were dehydrated in an ethanol series and embedded in paraffin. Sections (8-10 µm thick) were cut with a Jung Multicut 2045 microtome (Leica, Nussolch, Germany) and used for immunostainings. Sections were deparaffinized with xylene, rehydrated in an ethanol series and were then blocked with a solution of 2% BSA and 0.1% Tween in PBS for 30 min and subsequently incubated with anti-Gabarap antibody (1:250) for 2 hours at room temperature. After washing with PBS, sections were incubated for 1 hour with a Cy5-conjugated rabbit antibody (Abcam) at a concentration of 1:100. Samples were observed using a Nikon Eclipse Ni-U fluorescence microscope (Nikon, Tokyo, Japan). Images were acquired with a Nikon DS-5 M-L1 digital camera system (Nikon).

2.7 Acid phosphatase activity assay

Midgut dissection and storage was performed as described above for qRT-PCR samples. Midguts were dissected on ice and, after a rinse in a sterile Saline Solution for Lepidoptera (SSL) (210 mM sucrose, 45 mM KCl, 10 mM Tris–HCl, pH 7.0), were stored in liquid nitrogen until use. After being thawed, midguts were homogenized in 10 µl/µg of tissue of the following homogenization buffer: 100 mM mannitol, 10 mM HEPES-Tris at pH 7.2. A protease inhibitor cocktail (Thermo Fisher Scientific) was added freshly before the homogenization procedure. The protein concentration in the homogenates was determined using the Bradford assay (Bradford, 1976), with BSA as a standard. The enzyme activity in the homogenates was assayed in a reaction volume of 250 µl of 7.6 mM 4-nitrophenyl phosphate in citrate buffer (45.9 mM, pH 4.9) for 30 min, according to the method reported by Moss (1983). The reaction was performed at 25 °C and stopped by adding 1 ml of 0.1 M sodium hydroxide. Color development was determined at 405 nm using an Infinite F200 96-well plate-reader (Tecan, Männedorf, Switzerland). Each value was the result of experiments performed on 3 to 6 series of midguts. Statistical analysis was performed using Student's *t*-test or Anova followed by Tukey HSD test.

2.8 Analysis of caspase release

For the detection of caspase release, yellow body were extracted from pupal midguts, added to one volume of SSL and centrifuged for 5 min at 100 x g to separate the cells from the extracellular content. The two fractions (pellet and supernatant) were added to 100 µl of RIPA buffer, incubated for 1 hour and centrifuged at

15000 x g for 15 min at 4 °C. The supernatant was recovered and the proteins were quantified. Immunoblotting of BmCaspase-1 and BmGapdh was performed using the same protocol described in the "western blot analysis" section. In this experiment, anti-Gapdh was not used as a loading control (Franzetti et al., 2012) but rather as a marker to verify appropriate manipulation of the yellow body cells.

2.9 Light microscopy (LM), transmission electron microscopy (TEM), and scanning electron microscopy (SEM)

Midguts were dissected and fixed overnight in 4% glutaraldehyde in 0.1 M sodium cacodylate buffer, pH 7.2 at 4 °C. Specimens were then postfixed in 1% osmium tetroxide for 1 hour, dehydrated in an ethanol series, and embedded in an Epon/Araldite 812 mixture. Semithin (0.75 µm) and thin (70 nm) sections were obtained using a Leica Reichert Ultracut (Leica). Sections were stained with crystal violet and basic fuchsin and observed by using a Nikon Eclipse Ni-U microscope. Images were acquired with a Nikon DS-5M-L1 digital camera system. Thin sections were mounted on copper grids (200 meshes), stained using uranyl acetate and lead citrate and observed by using a Jeol JEM-1010 electron microscope (Jeol, Tokyo, Japan). Images were acquired by an Olympus Morada digital camera.

For SEM analysis, yellow body cells extracted from pupal midguts were fixed with 1% glutaraldehyde in 0.1 M Na-cacodylate buffer and postfixed in a solution of 1% osmium tetroxide and 1.25% potassium ferrocyanide for 1 hour at room temperature. Samples were embedded in polyfreeze cryostat embedding medium and stored at -80 °C; cryosections were washed in PBS and postfixed in the same solution of 1% osmium tetroxide and 1.25% potassium ferrocyanide for 30 min. Samples were washed in PBS

and then immersed in 0.1% osmium tetroxide in PBS for 48 hours. Slices were dehydrated in an increasing series of ethanol and subjected to critical point drying with CO_2. Dried slices were mounted on stubs, gold coated with a sputter K250 coater, and then observed with a Philips SEM-FEG XL-30 microscope (Philips, Eindhoven, The Netherland).

3 RESULTS

3.1 Analysis of autophagy in the midgut of B. mori *during metamorphosis*

In a previous work from our group (Franzetti et. al., 2012), the presence of autophagic features in the midgut of *B. mori* during metamorphosis was reported. On the other hand, the precise timing of autophagy activation was only hypothesized. To overcome this limit, we first analyzed the expression of some autophagic genes at different time points by qRT-PCR, starting from fifth larval instar up to the pupal stage. In particular, we evaluated the expression of *BmATG8*, a gene encoding an autophagosomal protein that is routinely used as a marker of the autophagic flux, and *BmATG1*, a gene encoding a regulatory protein that is considered the most upstream activator of autophagosome formation. *BmRP49* was used as a reference for the analysis since, in preliminary experiments, it demonstrated to be stable across the whole sample range. The levels of *BmATG8* mRNA started to increase from W stage and reached a peak of expression at SD1 (Fig. 8A). The levels of *BmATG1* mRNA showed a pattern similar to that of *BmATG8* until SD1. After a decrease at SD2 and PP stage, *BmATG1* expression showed a new maximum during the first days of the pupal stage (P3) (Fig. 8B). Since the analysis of the mRNA expression levels of the two genes confirmed the activation of autophagy in the midgut during metamorphosis, we monitored the autophagic flux by using a specific marker, i.e., Atg8. To this aim, we assayed a commercial anti-Gabarap antibody as a tool to recognize both BmAtg8 and BmAtg8-PE in *B. mori*. This antibody was selected for two reasons: i) BmAtg8 belongs to the Gabarap protein family; ii) sequence alignment of HsGabarap (NP_009209.1) and BmAtg8 (NP_001040244.1) proteins showed

91% identity (Fig. 9A). Western blot analysis demonstrated that the antibody specifically reacted with a *B. mori* Atg8 recombinant protein produced by using BL21DE3/pET28+BmAtg8 bacteria, and detected a 16 kDa band. On the other hand, the antibody did not recognize any proteins in BL21DE3/pET28 negative control bacteria. By testing protein extracts obtained from silkworm midgut, the antibody recognized a 16 kDa band (BmAtg8), as well as a second 14 kDa band (BmAtg8-PE). The antibody proved to be very specific and no additional bands were detected at molecular weights other than those reported (Fig. 9B). Western blot analysis of midgut samples at different time points showed an increase in the levels of BmAtg8-PE at SD2 stage (Fig. 9C), with a delay of about 24 hours compared to the pattern observed for *BmATG8* mRNA expression (Fig. 8A). After PP stage, the expression of the protein dropped significantly. It is important to note that BmAtg8 did not show the same expression pattern of BmAtg8-PE: in fact, this protein was detected at relatively high levels already at larval stage, while it decreased during the pupal stage. Immunostainings evidenced the localization of BmAtg8 on the autophagosomal compartments. In fact, BmAtg8-positive puncta were observed in the midgut epithelium during SD2, thus demonstrating the presence of autophagic vesicles in the midgut tissue at this developmental stage (Fig. 9E). Conversely, scarce BmAtg8-positive puncta were visible in L5D5 samples (Fig. 9D). TEM analysis confirmed the presence of a significant amount of autophagosomes at SD2. In fact at this stage abundant structures delimited by a double membrane, and containing cytoplasmic material and organelles, were identified in midgut cells (Fig. 9F), while these compartments were very rare during the larval stage (L5D5). The analysis of the activity of acid phosphatase confirmed an involvement of lysosomes in this setting. In detail, the activity of this enzyme increased from W stage, reached a peak during SD2

and then decreased at PP stage (Fig. 9G), thus overlapping the trend observed in the BmAtg8-PE expression.
Collectively, these data demonstrate that the transcriptional induction of the autophagic process in *B. mori* midgut starts at W-SD1 stage. Moreover, the highest levels of autophagy are observed at SD2 stage, as indicated by the expression of BmAtg8-PE and the activity of acid phosphatase.

3.2 Analysis of apoptosis in the midgut of B. mori *during metamorphosis*

Franzetti et al. (2012) reported a co-existence of autophagic and apoptotic features during the degeneration of the larval midgut in *B. mori*. We thus analyzed different apoptotic markers to better characterize apoptosis in the midgut cells undergoing degeneration. In particular, we evaluated the mRNA expression of an effector caspase, *BmCASPASE-1*, and an initiator caspase, *BmCASPASE-5*. Caspase-1 is the homolog of *Drosophila* Drice and Dcp-1, and is thus considered the main effector caspase in Lepidoptera (Courtiade et al., 2011). Caspase-5, on the other hand, is the lepidopteran homolog of *Drosophila* Dronc (Courtiade et al., 2011), an essential initiator caspase involved in developmental apoptosis and highly transcribed during metamorphosis (Cakouros et al., 2004; Daish et al., 2004). *BmCASPASE-1* gene was strikingly upregulated during W-SD1, compared to the last larval stage. The expression of this gene strongly decreased during SD2, but reached a second, lower peak during the first day of the pupal stage (P1). *BmCASPASE-1* gene expression then slowly decreased during the following pupal days (Fig. 10A). The expression pattern of the initiator caspase *BmCASPASE-5* resembled that of *BmCASPASE-1* with two peaks at W and P1 stage. However the increase in mRNA levels of

BmCASPASE-5 during W stage was lower than *BmCASPASE-1* (~4 folds versus ~35 folds) (Fig. 10B). Since the production of active caspases requires the cleavage of a zymogen (procaspase), we evaluated the expression levels of both uncleaved and cleaved BmCaspase-1 protein in midgut cells. The anti-cleaved Caspase-3 antibody used in this work was already described to recognize *Drosophila* caspases in previous studies (Baum et al., 2007; Fan and Bergman, 2010; Xu et al., 2008). Among *B. mori* caspases, the epitope recognized by the antibody (ETD; Fan and Bergman, 2010) was present only within BmCaspase-1 sequence (Fig. 10C). The protein detected by the antibody in protein extracts obtained from silkworm midgut was at the expected molecular weight (17 kDa), confirming the specificity of this antiserum for cleaved Caspase-1, and making us confident about its use to recognize the protein of our interest. The antibody used to recognize the uncleaved form of BmCaspase-1 detected a 25 kDa band, that was comparable with the expected molecular weight of the inactive p25 Caspase-1 intermediate (Liu et al., 2005). No expression of cleaved BmCaspase-1 could be observed in midgut tissues until SD2 stage. The activated effector caspase was highly expressed at PP stage, while, after a decrease at P1, it increased again at P3. No caspase activity was detected during the last pupal days (Fig. 10D). This pattern of activation was very similar, although delayed of about 48 hours, to that of *BmCASPASE-1* mRNA (Fig. 10A). On the other hand, the uncleaved BmCaspase-1 form (p25) could be detected since W stage up to P3 (Fig. 10E).

These data collectively show that the transcriptional induction of the apoptotic machinery occurs at W-SD1 stage. Starting from W stage, the presence of uncleaved BmCaspase-1 can be detected in the midgut tissues. However the strong activation of this effector caspase is observed only 48 hours later, at PP stage.

Subsequently, a lower peak of caspase expression and activation is visible at P1 and P3 stage, respectively.

Under *in vivo* conditions, apoptotic cells are usually removed by professional phagocytes. When they are not available, the natural outcome of apoptosis is secondary necrosis. The release of caspases in the extracellular environment is considered an undisputable marker of secondary necrosis (Silva et al., 2010). Given that phagocytes were not observed in midgut lumen, we hypothesized that degenerating cells within the yellow body undergo secondary necrosis. This hypothesis was verified by SEM analysis that showed membrane ruptures in yellow body cells (P3 stage) (Fig. 11A). Moreover, we tested whether these cells released activated caspases in the lumen of the new pupal midgut, where they are localized. Cleaved BmCaspase-1 was observed both inside and outside of the yellow body cells. A differential signal for Gapdh in the two fractions (cells and supernatant) demonstrated that the release of caspases was not due to technical artifacts (i.e., inappropriate manipulation of the cells that could break them and mix the inner and outer cell compartment) (Fig. 11B).

In summary, we can conclude that in *B. mori* midgut the induction of autophagy (SD1-SD2 stage) precedes caspase activation of 24-48 hours (PP stage). Apoptosis remains active during the following pupal days and a second pulse of caspase activation is observed at P3 stage. Once apoptosis is activated, degenerating cells within the yellow body undergo secondary necrosis and release their cytoplasmic content within the lumen of the pupal midgut.

3.3 Regulation of autophagy by 20E

20E is one of the major regulators of development in insects and it has been linked to the induction of autophagy in the silkworm fat

body (Tian et al., 2013). As described above, we observed that the transcription of autophagic genes is triggered concurrently with the increase of 20E titer in the hemolymph (commitment peak) (Satake et al., 1998; Truman and Riddiford, 1999). However, a causal relationship between the two events in midgut needed to be proved. We therefore analyzed the mechanism of induction of autophagy by ecdysone in this tissue, by injecting fifth instar larvae with 20E. According to preliminary assays in which different amounts of 20E were tested (1-50 µg/larva), we decided to inject 10 µg/larva in the following experiments. This was, in fact, the lowest amount of 20E able to induce a strong pigmentation of the silk-spinning apparatus (spinneret), cessation of feeding and gut purging once injected in fifth instar larvae. These effects were identical to those observed in larvae at wandering stage, when the physiological 20E peak occurs. To verify if the autophagic process was transcriptionally activated by 20E administration, we measured the expression of *BmATG1* and *BmATG8*. The expression of *BmATG8* was upregulated 6 hours after the hormone injection but returned to levels comparable with the controls 24 and 48 hours following the treatment (Fig. 12A). The levels of *BmATG1* mRNA were increased both 6 and 24 hours after the treatment with 20E. 48 hours after the injection, the expression decreased to a level lower than the controls (Fig. 12B). Since these experiments confirmed the overexpression of *ATG* genes following 20E treatment, we analyzed the expression of Atg8-PE to assess whether the autophagic process was activated by the hormone injection. A strong increase of BmAtg8-PE was observed 6 and 24 hours after the hormone treatment (Fig. 12C). The complete induction of autophagy was confirmed by measuring the activity of acid phosphatase, which increased 24 and 48 hours following the treatment (Fig. 12D). From these experiments we can conclude that 20E is able to upregulate *ATG* genes and activate the

autophagic flux. In the literature it is reported that 20E dephosphorylates the protein Tor both in *Drosophila* and *B. mori* fat body, thus eliciting the induction of the autophagic process (Rusten et al., 2004; Tian et al., 2013). However it was also reported that 20E can activate autophagy acting independently from Tor pathway inhibition (Tian et al., 2013). In order to verify an involvement of the Torc1 complex in the 20E-induced autophagic process in midgut cells, we evaluated the activity of this complex by measuring the phosphorylation levels of its target, 4ebp1. Western blot analyses showed that Torc1 activity significantly decreased after the treatment of the larvae with 20E. These data demonstrate that the induction of autophagy by 20E is mediated by Torc1 (Fig. 12E). To verify whether the effect of 20E is achieved exclusively through Torc1 recruitment, we evaluated the effects of the inhibition of this complex on the induction of autophagy. To this aim we injected rapamycin (10 µg/larva) (Tian et al., 2013). The levels of phosphorylated 4ebp1 showed a strong decrease, similar to that observed after the injection of 20E, both 6 and 24 hours after rapamycin administration, confirming that the treatment was effective (Fig. 13A). Injection of rapamycin during the last larval instar determined an increase in the expression of *BmATG8* at 6 and 24 hours after the administration (Fig. 13B). On the other hand, rapamycin was not able to induce the expression of *BmATG1* (Fig. 13C). Surprisingly, BmAtg8-PE levels showed a decrease 6 hours following the treatment and even a more pronounced effect was observed after 24 hours (Fig. 13D). The activity of acid phosphatase did not show a significant increase after rapamycin injection (Fig. 13E), confirming the occurrence of an incomplete autophagic response.

From these data we can conclude that 20E acts on more than one targets, comprising Torc1, to regulate autophagy.

3.4 Regulation of apoptosis by 20E

Similarly to *ATG* genes, we observed that also the transcription of apoptotic genes was upregulated during metamorphosis in concomitance with the rise of 20E titer in the hemolymph (Satake et al., 1998; Truman and Riddiford, 1999). Manaboon et al. (2008) hypothesized that, in the silkworm anterior silk gland, the first pulse of ecdysone (commitment peak) is able to stimulate a genomic response (upregulation of apoptotic gene transcription), while the second pulse (metamorphic peak) activates a non-genomic response of apoptosis (activation of caspases). To study the effects of 20E on the apoptotic induction in midgut cells, we conceived a set of experiments based on the injection of this hormone (10 µg/larva) during the last larval instar. The injection of a single dose of 20E led to the upregulation of *BmCASPASE-1* gene 6 hours later. 24 hours after the administration of 20E the mRNA levels of this gene decreased, remaining however higher than the controls. 48 hours following the treatment, gene expression returned to levels comparable to control larvae (Fig. 14A). On the other hand, no appreciable upregulation of the initiator caspase gene, *BmCASPASE-5*, was observed after ecdysone treatment (Fig. 14B). Given the transcriptional pattern of *BmCASPASE-1* following 20E administration, we decided to analyze the activation of this effector caspase at a protein level. A single dose of 20E was not able to activate this caspase, up to 72 hours following the injection, in none of the treated larvae (Fig. 14C). These data clearly show that, under physiological conditions, the 20E commitment peak can upregulate *BmCASPASE-1* expression, but it cannot activate BmCaspase-1 protein. To confirm the hypothesis that apoptosis is induced by the 20E pupal peak, we conceived an injection protocol to mimic the physiological pattern of ecdysone levels that occurs in the larva during metamorphosis:

to this aim we performed a second injection of 20E (50 µg/larva) 24 hours after the first hormone administration. Although different concentrations of hormone were tested (10-100 µg/larva), this amount was chosen to obtain a significant rise in 20E titer in the hemolymph and to reproduce the 20E metamorphic peak, without any toxic effects. As a result of the double administration of 20E, a strong activation of BmCaspase-1 was observed in 30% of the larvae. On the contrary no expression of caspases was observed in any of the larvae treated with a single injection of 20E (10 µg or 50 µg 20E/larva) (Fig. 14D). Our data confirm that, during metamorphosis, the first rise in 20E titer within the hemolymph (commitment peak) is needed to upregulate the expression of apoptotic genes, while activation of caspases is triggered only after the occurrence of the second 20E peak (metamorphic peak).

3.5 Role of autophagy in midgut degeneration

In the silkworm midgut, as in other developmental contexts, autophagy precedes apoptosis but its role as a pro-survival or pro-death mechanism is still a matter of debate. To get insights into the role of this process in degenerating midgut cells, we inhibited autophagy by using chloroquine. Chloroquine is a widely used autophagy inhibitor acting on the lysosome-autophagosome fusion step, thus blocking the autophagic flux. Different amounts of this inhibitor were tested (100 µg - 2 mg/larva) and 1 mg/larva was assessed to be the highest concentration that could be used without the induction of any toxic effects, such as mortality of the larvae and/or abnormal development of the pupal midgut epithelium. Larvae were injected at the beginning of autophagy activation (SD1 stage). TEM analysis performed on larvae treated with chloroquine showed an accumulation of a great quantity of vesicles in midgut cells, 72 hours after the administration (Fig.

15B) compared to controls (P1 stage) (Fig. 15A). According to their size, morphology and content, they could be classified as autophagy-related structures (Fig. 15C). Moreover, Atg8-PE levels (Fig. 15D), as well as the activity of acid phosphatase (Fig. 15E), increased in treated larvae compared to controls. These results demonstrate the efficacy of chloroquine in blocking the autophagic flux in midgut tissues and the consequent accumulation of both autophagosome and lysosomes in these cells. While the morphology of the new pupal epithelium did not show any difference in larvae injected with chloroquine, the organization of the yellow body appeared different between control and treated larvae. In fact, although the yellow body of control pupae underwent degeneration, its overall structure was still partially conserved (Fig. 15F). On the other hand, in treated larvae, the old epithelium showed a higher degree of degeneration than controls and no tissue structure was retained (Fig. 15G). Furthermore, western blot analysis showed an increase in the levels of cleaved BmCaspase-1 in larvae treated with the autophagy inhibitor (Fig. 15H).

The data collected demonstrate that inhibition of autophagy determines the accumulation of higher levels of caspases and a stronger degeneration of midgut cells. This suggests a pro-survival role of autophagy in this larval tissue.

3.6 Role of apoptosis in midgut degeneration

Apoptosis is considered the key player of tissue degeneration during development. On the other hand, activation of caspases is not always necessary for the removal of larval organs during insect metamorphosis (Denton et al., 2009). In order to collect information on this aspect, we blocked the activation of caspases by using z.vad.fmk, a pan-caspase inhibitor. This chemical is able

to selectively and irreversibly inhibit the activity of both initiator and effector caspases, thus blocking most of the apoptotic responses. Larvae were injected at SD1 or SD2 stage, just before the activation of BmCaspase-1, and the effects were evaluated at PP, P1 P3 and P9 stage. In preliminary assays, cleaved BmCaspase-1 was used as a marker to assess the best concentration of z.vad.fmk to be used in the following experiments. 25 µg/larva was chosen as the lowest amount of inhibitor able to completely suppress the activation of BmCaspase-1 (Fig. 16A). Neither mortality nor toxic effects were observed in larvae injected with this dose of z.vad.fmk. Larvae treated at SD2 with the caspase inhibitor showed undetectable levels of cleaved BmCaspase-1 24, 48 and even 96 hours after the treatment (PP, P1 and P3 stage, respectively) (Fig. 16B). TEM analysis revealed the presence of a limited number of apoptotic nuclei in these larvae (Fig. 16E) compared to controls (Fig. 16D), thus confirming a strong and specific inhibition of apoptosis after the treatment with z.vad.fmk. On the other hand, we observed an incomplete inhibition of caspases at PP stage when the larvae were treated with the inhibitor at SD1 stage (Fig. 16C). These results indicate that z.vad.fmk loses most of its activity within 24 hours after the injection, thus demonstrating that the timing of the treatment is crucial. The inhibition observed at 48 and 96 hours, in larvae treated at SD2 stage, can not be therefore explained by the persistence of z.vad.fmk in the hemolymph. Consequently, we hypothesize that the caspase activity observed during the pupal stage completely depends on the first wave of caspase activation that occurs at PP stage.

A significant alteration in the appearance of the larval midgut epithelium was visible in larvae treated with z.vad.fmk at SD2. In fact, while in control P3 pupae (Fig. 16F) the larval epithelium clearly showed a degenerated morphology, this tissue still

possessed an epithelial-like structure in treated animals (Fig. 16G). The effect of caspase inhibition was even stronger at P9 stage. In fact, while in control larvae (Fig. 16H) only debris and small cell clusters undergoing degeneration were visible, larvae injected with z.vad.fmk still retained a larval midgut characterized by epithelial-like morphology (Fig. 16I). The morphology of the new pupal epithelium was comparable in control and treated animals, and no alteration was observed in the latter. Our experiments collectively demonstrate that apoptosis is the key process that drives larval midgut degeneration during silkworm metamorphosis.

4 DISCUSSION

Previous work has described the occurrence of autophagy and apoptosis in the larval organs of Lepidoptera (Franzetti et al., 2012; Khoa and Takeda, 2012; Tettamanti et al., 2007; Tian et al., 2012; Tian et al., 2013). However the role of autophagy, as well as its relationship with apoptosis, are troublesome and still a subject of debate. This is mainly due to the fact that the two processes show peculiar features in tissues and organs of these insects and their role seems to be context-dependent. With the aim to overcome this gap of knowledge, we analyzed the timing of occurrence of autophagy and apoptosis during the demise of silkworm midgut. Moreover, we performed functional experiments, by using activators and inhibitors of the two processes, to get insights into their regulatory mechanisms. To our knowledge this is the first study that investigates in detail both autophagy and apoptosis, their regulation, as well as their functional relationship in an *in vivo* lepidopteran model.

4.1 Autophagy and apoptosis are activated during the degeneration of the larval midgut

The appropriate criteria to assess the activation of autophagy are often a matter of debate, especially when unconventional model systems are used. In fact, there are no absolute criteria for determining autophagic status that are applicable in every biological or experimental context (Klionsky et al., 2012). In order to assess the activation of autophagy and to follow the autophagic flux during metamorphosis, we tested different direct (expression of Atg8-PE) and indirect (mRNA expression of *ATG* genes and activity of acid phosphatase) markers in *B. mori* midgut.

We demonstrated that the transcriptional activation of two key *ATG* genes (*BmATG1* and *BmATG8*) in this organ occurs at the beginning of metamorphosis. In previous studies on silkworm midgut, the upregulation of autophagy-related genes was correlated with a response to starvation induced by cessation of feeding, which takes place at the end of the last larval instar (Casati et al., 2012; Franzetti et al., 2012). In particular, here we show that, following the upregulation of the genes belonging to the autophagic machinery is triggered, the autophagic flux is activated. So, even though Klionsky et al. (2012) in their guidelines on autophagy reported that assessing the mRNA levels of autophagy-related genes may provide only correlative data related to the induction of autophagy, our results confirm that, in our experimental model, the overexpression of *ATG* genes precedes the induction of autophagy and can be therefore considered as an indirect marker of this process at least in some settings. In addition, our data confirm that autophagy is involved in the developmental remodeling of *B. mori* midgut during metamorphosis, as shown also for *H. virescens* (Tettamanti et al., 2007), *M. sexta* (Muller et al., 2004) and *Drosophila* (Denton et al., 2009) midgut, as well as other silkworm organs (Li et al., 2010; Tian et al., 2013).

The analysis of caspase mRNA levels performed in the current work demonstrates that apoptosis is activated at transcriptional level concomitantly with the upregulation of *ATG* genes. Conversely, the activation of effector caspases is observed only from the prepupal stage. Moreover a consequent, but lower, rise of transcriptional and functional activation of apoptosis is observed during the first days of the pupal stage. We hypothesize that the presence of two rounds of caspase activation could be due to a differential timing in the demise of different midgut regions or cell types (e.g., columnar vs. goblet cells). This hypothesis is

corroborated by a previous study on the midgut of *Galleria mellonella*, where three different apoptotic waves, necessary for the degeneration of distinct parts of the midgut epithelium, were reported (Khoa et al., 2012).

Although in silkworm the apoptotic process is characterized by typical features such as the activation of caspases, DNA fragmentation and nuclear pyknosis, we did not find any evidence of phagocytes that can remove apoptotic bodies in the midgut tissues (Franzetti et al., 2012). For this reason, we hypothesized that the final demise of yellow body cells could occur by secondary necrosis, a process that represents the natural outcome of apoptosis when scavengers are not available to remove apoptotic bodies. Generally this process occurs *in vivo* when apoptotic cells are localized in territories topologically outside the organism, such as the gut or the airway lumen and is characterized by damage of plasma membrane and terminal cell disintegration (Silva, 2010). In silkworm midgut, the rupture of cell membrane and the release of activated caspases from damaged yellow body cells in the outer environment are undisputable evidence of secondary necrosis (Silva, 2010), thus substantiating our hypothesis. Due to the loss of membrane integrity, yellow body cells release their cytoplasmic content, which is essentially composed of debris and products of cell degradation generated by death processes, in the extracellular environment, i.e., the lumen of the new pupal-adult midgut. Released molecules are thus made available for absorption by the newly forming pupal midgut (Franzetti et al., 2015).

4.2 20E regulates both autophagy and apoptosis during metamorphosis

20E is usually regarded as a regulator of autophagy in various insect models. Similarly to what happens in the *Drosophila* fat

body (Rusten et al., 2004), it was demonstrated that autophagy can be stimulated by 20E in the fat body of *B. mori*: this hormone is able to increase autophagy by inhibiting the Tor pathway, thus allowing the activation of the downstream Atg1 complex (Tian et al., 2013).

Our results demonstrate that 20E can trigger autophagy in the midgut of *B. mori* during metamorphosis. In particular, the activation of autophagy is mediated by the first rise of 20E in the hemolymph (20E commitment peak). We also demonstrate that Torc1 is involved in the molecular response to 20E, similarly to what happens in *Drosophila* (Rusten et al., 2004) and *B. mori* (Tian et al., 2013) fat body. Anyway, Torc1 inhibition alone is not sufficient to activate a full autophagic response, suggesting that 20E acts concurrently on more than one targets. Unlike 20E, rapamycin fails in stimulating the expression of *BmATG1*. This result is consistent with the presence of an Ecdysone Response Element in the promoter of this gene (Tian et al., 2013), that likely permits its transcriptional regulation without the involvement of the Tor pathway. For these reasons, we hypothesize that Torc1 is involved in the activation of autophagy, but it can not induce the production of all the components needed for a full autophagic response. Thus, following rapamycin treatment, the autophagic flux is activated and BmAtg8-PE, previously localized on autophagosomal membranes, is degraded within autolysosomes; in this setting, since no *de novo* synthesis of autophagosomes occurs after the depletion of one or more autophagic components, the final outcome is an overall decrease in the BmAtg8-PE levels. These results demonstrate that for a proper evaluation of autophagic markers, such as BmAtg8-PE, it must be considered that autophagy is a dynamic and multi-step process that can be modulated at different points. In accordance with our results, Tian et al. (2013) showed that injection of rapamycin in feeding larvae

moderately induces autophagy, but the effects elicited are weaker than those obtained by 20E administration. Also in that case the authors hypothesized that the insufficient upregulation of some critical *ATG* genes by rapamycin injection was responsible for this outcome. In addition, reduced Atg8-PE levels were also observed in Sl-HP lepidopteran cells where autophagy was induced by amino acid starvation. The authors hypothesized that starvation does not induce autophagosome formation in these cells, but accelerates autophagosome–autolysosome maturation (Gai et al., 2013).

Since the temporal pattern of the apoptotic process differed from that of autophagy, we conceived a set of experiments to investigate the role of 20E in the regulation of apoptosis. Our results show that a single 20E administration is able to upregulate *BmCASPASE-1*, confirming a role for this hormone in the transcriptional regulation of apoptosis. On the contrary, since no upregulation of *BmCASPASE-5* was observed after the hormonal treatment, we hypothesize that its transcription could be regulated *in vivo* by a different stimulus or other factors are needed for 20E to be effective on this gene. The analysis of activated caspase demonstrated that the administration of a single dose of 20E can not trigger apoptosis, while the injection of two subsequent doses of 20E, that mimic commitment and metamorphic peak, is needed to induce the cleavage and the activation of the effector caspase, and to achieve a full apoptotic response. Taken together, our data demonstrate that the first 20E pulse activates the transcriptional regulation of apoptotic genes and the translation of caspases; thereafter a 20E metamorphic peak is necessary to stimulate the activation of effector caspases (Fig. 17). Manaboon et al. (2008) proposed a similar model for anterior silk gland degeneration during metamorphosis, in which PCD was transcriptionally triggered by the commitment peak, while the pathway that leads to caspase activation was induced by the pupal 20E rise. An

involvement of 20E in the induction of apoptosis during metamorphosis was also described in the silkworm fat body (Tian et al., 2012). However, in that case a single administration of 20E was sufficient to activate the apoptotic response. It is important to note that the degeneration of larval tissues during metamorphosis shows a specific temporal frame in each organ. Moreover, while some organs are completely degraded during metamorphosis (e.g., larval midgut, silk gland), some others are simply remodeled (e.g., fat body). So, it is likely that each organ responds to hormonal stimuli according to the expression levels of hormone receptors or other components of the hormone responsive pathway.

4.3 Role of autophagy and apoptosis

In *Drosophila* the regulation, as well as the role, of autophagy and apoptosis is reported to be highly context-specific. For example, cell death in the abdominal muscles occurs by apoptosis and does not require autophagy (Zirin et al., 2013) Apoptosis was also initially regarded as the major force driving the demise of the midgut (Yin and Thummel, 2004), although, a subsequent work pointed out autophagy as the indispensable process needed for the degeneration of this organ, while caspase activity appears dispensable (Denton et al., 2009). In the removal of salivary gland and during oocyte maturation, autophagy was reported to be necessary for the activation of a caspase-dependent cell death (Berry and Baehrecke, 2007; Nezis et al., 2010). Also in Lepidoptera, the function of autophagy and apoptosis was hypothesized to be tissue-specific (Franzetti et al., 2012; Khoa and Takeda, 2012; Khoa et al., 2012; Tian et al., 2012; Tian et al., 2013). On the other hand, functional studies aiming at unraveling the role and the relationship between the two processes within the

same insect model have never been performed. Our data on silkworm midgut demonstrate that the inhibition of the autophagic flux does not impair either the demise of the cells or the activation of caspases. Thus autophagy is not needed for the activation of apoptosis in this setting. Conversely, the epithelium of larvae treated with the autophagy inhibitor shows a more degraded morphology and an enhanced level of caspases, compared to controls. Thus, these data corroborate the evidence obtained in previous studies by our group (Franzetti et al., 2012; Franzetti et al., 2015) and suggest a dual role for autophagy in the midgut: i) it permits larval midgut cells to survive to starvation during early metamorphosis; ii) it allows the catabolic degradation of the cell components that can be later used by the newly forming pupal-adult epithelium. In fact, Franzetti et al. (2012; 2015) proved that autophagy is responsible for the production of high ATP levels in the midgut during metamorphosis and that the new midgut epithelium is able to recycle and absorb molecules derived from the degeneration of the old larval midgut. Moreover, the involvement of autophagy in the catabolic response triggered by starvation and necessary to produce energy during metamorphosis was proposed also in the fat body (Tian et al., 2013). Accordingly, if autophagy is inactivated at this developmental stage, cells can not cope with the absence of nutrients, and a higher degree of degeneration of the midgut tissue is observed. We can speculate that this inability of the cells to counteract the lack of nutrients, due to the inhibition of autophagy, can trigger other death-related mechanisms (e.g., necrosis). This hypothesis is supported by a work on *B. mori* Bme cells, where the inhibition of starvation-induced autophagy by 3-methyladenine leads cells to necrotic-like cell death instead of apoptosis (Wu et al., 2011). Unraveling the mechanisms that underlie the effects determined by the inhibition of autophagy would lead to better understand the relationship

between energy balance, autophagy and cell death in this experimental model.

The results obtained in our study also confirm that the major process that is responsible for the degeneration of the larval midgut during metamorphosis is apoptosis. In fact, *in vivo* inhibition of caspases strongly delays the demise of the larval epithelium. Our data also show how activation of apoptosis is finely regulated, since it can be achieved only in a very short window of time (PP stage). Indeed, active effector caspases are never observed in midgut tissues before PP stage. Moreover, if the prepupal wave of caspase activation is chemically inhibited, the effector caspases can not be activated during the pupal stage anymore.

In summary, we demonstrated that, under physiological conditions, the first rise of 20E stimulates the transcriptional activation of both autophagic and apoptotic genes. Autophagy is subsequently activated, allowing the cells to survive under conditions of nutrient deprivation and taking part to the degradation of the cell components. On the other hand, apoptosis is switched on 24-48 hours after the onset of autophagy by the pupal rise of 20E and it leads to the demise of the cells in a well-regulated manner until the pupal stage. Apoptotic cells undergo secondary necrosis and their content is released in the lumen of the pupal-adult midgut, where it is progressively absorbed by the new epithelium (Fig. 17).

5 CONCLUSIONS

1. Autophagy precedes apoptosis during the degeneration of the larval midgut in *B. mori*.

2. Autophagy is activated at the beginning of metamorphosis in response to the 20E commitment peak. 20E acts on different targets, including Torc1, to induce autophagy.

3. Autophagy is involved in the survival of the larval epithelium during W-SD2 stage and in the catabolic degradation of the cell components that are later absorbed by the adult epithelium.

4. Apoptosis is transcriptionally activated at the beginning of metamorphosis following the 20E commitment peak. Activation of effector caspases is triggered by the 20E pupal peak.

5. Apoptosis is the key process responsible for the demise of the larval midgut epithelium.

6 REFERENCES

Ahmad M, Srinivasula SM, Wang L, Litwack G, Fernandes-Alnemri T et al., (1997). *Spodoptera frugiperda* caspase-1, a novel insect death protease that cleaves the nuclear immunophilin FKBP46, is the target of the baculovirus antiapoptotic protein p35. J Biol Chem. 272:1421-1424.

Baldwin KM, Hakim R, Loeb M, Sadrud-Din S, (1996). Midgut development. In: Lehane M.J., Billingsley P.F. (Eds) Biology of the insect midgut. Chapman and Hall, London, pp 31-54.

Baum JS, Arama E, Steller H, McCall K, (2007). The *Drosophila* caspases Strica and Dronc function redundantly in programmed cell death during oogenesis. Cell Death Differ. 14:1508–1517.

Bejarano E, Cuervo AM, (2010). Chaperone-mediated autophagy. Proc Am Thorac Soc. 7:29-39.

Berry DL, Baehrecke EH, (2007). Growth arrest and autophagy are required for salivary gland cell degradation in *Drosophila*. Cell. 131:1137-1148.

Bradford MM, (1976). A rapid and sensitive method for the quantitation of microgram quantities of protein utilizing the principle of protein-dye binding. Anal Biochem. 72:248-254.

Buszczak M, Cooley L, (2000). Eggs to die for: cell death during *Drosophila* oogenesis. Cell Death Differ. 7:1071-1074.

Cai MJ, Liu W, Pei XY, Li XR, He HJ et al., (2014). Juvenile hormone prevents 20-hydroxyecdysone-induced metamorphosis by egulating the phosphorylation of a newly identified broad protein. J Biol Chem. 289:26630-26641.

Cakouros D, Daish TJ, Kumar S, (2004). Ecdysone receptor directly binds the promoter of the *Drosophila* caspase dronc, regulating its expression in specific tissues. J. Cell Biol. 165:631–640.

Cappellozza L, Cappellozza S, Saviane A, Sbrenna G, (2005). Artificial diet rearing system for the silkworm *Bombyx mori* (Lepidoptera: Bombycidae): effect of vitamin C deprivation on larval growth and cocoon production. Appl Entomol Zool. 40:405-412.

Casati B, Terova G, Cattaneo AG, Rimoldi S, Franzetti E et al., (2012). Molecular cloning, characterization and expression analysis of ATG1 in the silkworm, *Bombyx mori*. Gene. 511:326-337.

Chang HY, Yang X, (2000). Proteases for Cell Suicide: Functions and Regulation of Caspases. Microbiol Mol Biol Rev. 64:821-846.

Chang YY, Neufeld TP, (2009). An Atg1/Atg13 complex with multiple roles in TOR-mediated autophagy regulation. Mol Biol Cell. 20:2004-2014.

Chen P, Rodriguez A, Erskine R, Thach T, Abrams JM, (1998). Dredd, a novel effector of the apoptosis activators reaper, grim, and hid in *Drosophila*. Dev Biol. 201:202-216.

Chen P, Abrams JM, (2000). *Drosophila* Apoptosis and Bcl-2 Genes: Outliers Fly in. J Cell Biol. 148:625–628.

Cheung WL, Ajiro K, Samejima K, Kloc M, Cheung P et al., (2003). Apoptotic phosphorylation of histone H2B is mediated by mammalian sterile twenty kinase. Cell. 113:507-517.

Coleman ML, Sahai EA, Yeo M, Bosch M, Dewar A et al., (2001). Membrane blebbing during apoptosis results from caspase-mediated activation of ROCK I. Nat Cell Biol. 3:339-345.

Conradt B, Horvitz HR, (1998). The C. elegans protein EGL-1 is required for programmed cell death and interacts with the Bcl-2-like protein CED-9. Cell. 93:519-529.

Courtiade J, Pauchet Y, Vogel H, Heckel DG, (2011). A comprehensive characterization of the caspase gene family in insects from the order Lepidoptera. BMC Genomics. 12:357.

Daish TJ, Mills K, Kumar S, (2004). *Drosophila* caspase DRONC is required for specific developmental cell death pathways and stress-induced apoptosis. Dev Cell. 7:909-915.

del Peso L, Gonzalez VM, Nunez G, (1998). *Caenorhabditis elegans* EGL-1 disrupts the interaction of CED-9 with CED-4 and promotes CED-3 activation. J Biol Chem. 273:33495-33500.

del Peso L, Gonzalez VM, Inohara N, Ellis RE, Nunez G, (2000). Disruption of the CED-9.CED-4 complex by EGL-1 is a critical step for programmed cell death in *Caenorhabditis elegans*. J Biol Chem. 275:27205-27211.

Denton D, Shravage B, Simin R, Mills K, Berry DL et al., (2009). Autophagy, not apoptosis, is essential for midgut cell death in *Drosophila*. Curr Biol. 19:1741–1746.

Denton D, Aung-Htut MT, Kumar S, (2013). Developmentally programmed cell death in *Drosophila*. Biochim Biophys Acta. 1833:3499-3506.

Deveraux QL, Reed JC, (1999). IAP family proteins - suppressors of apoptosis. Genes Dev. 13:239-252.

Dice JF, (1990). Peptide sequences that target cytosolic proteins for lysosomal proteolysis. Trends Biochem Sci. 15:305-309.

Dorstyn L, Mills K, Lazebnik Y, Kumar S, (2004). The two cytochrome c species, DC3 and DC4, are not required for caspase activation and apoptosis in *Drosophila* cells. J Cell Biol. 167:405–410.

Dow JAT, (1986). Solid/plant feeders: "phytophagous insects". In Insect midgut function. Advances in insect physiology; 19:222-327.

Eisenberg-Lerner A, Bialik S, Simon HU, Kimchi A, (2009). Life and death partners: apoptosis, autophagy and the cross-talk between them. Cell Death Differ. 16:966-975.

Enari M, Sakahira H, Yokoyama H, Okawa K, Iwamatsu A et al., (1998). A caspase-activated DNase that degrades DNA during apoptosis, and its inhibitor ICAD. Nature. 391:43–50.

Endo Y, Nishiitsutsuji-Uwo J, (1981). Gut endocrine cells in insects: the ultrastructure of the gut endocrine cells of the lepidopterous species. Biomed Res. 2:270-280.

Eskelinen EL, (2006). Roles of LAMP-1 and LAMP-2 in lysosome biogenesis and autophagy. Mol Aspects Med. 27:495-502.

Eskelinen EL, (2008). To be or not to be? Examples of incorrect identification of autophagic compartments in conventional transmission electron microscopy of mammalian cells. Autophagy. 4:257–260.

Eskelinen EL, Reggiori F, Baba M, Kovács AL, Seglen PO, (2011). Seeing is believing: the impact of electron microscopy on autophagy research. Autophagy. 7:935-956.

Fan Y, Bergmann A, (2010). The cleaved-Caspase-3 antibody is a marker of Caspase-9-like DRONC activity in *Drosophila*. Cell Death Differ. 17:534-539.

Franzetti E, Huang ZJ, Shi YX, Xie K, Deng XJ et al., (2012). Autophagy precedes apoptosis during the remodeling of silkworm larval midgut. Apoptosis. 17:305-324.

Franzetti E, Romanelli D, Caccia S, Cappellozza S, Congiu T et al., (2015). The midgut of the silkmoth *Bombyx mori* is able to recycle molecules derived from degeneration of the larval midgut epithelium. Cell Tissue Res. 361:509-528.

Fuentes-Prior P, Salvesen GS, (2004). The protein structures that shape caspase activity, specificity, activation and inhibition. Biochemical J. 384:201-232.

Gai Z, Zhang X, Islam M, Wang X, Li A et al., (2013). Characterization of Atg8 in lepidopteran insect cells. Arch Insect Biochem Physiol. 84:57-77.

Galluzzi L, Maiuri MC, Vitale I, Zischka H, Castedo M et al., (2007). Cell death modalities: classification and pathophysiological implications. Cell Death Differ. 14:1237-1243.

Galluzzi L, Vitale I, Abrams JM, Alnemri ES, Baehrecke EH et al., (2012). Molecular definitions of cell death subroutines: recommendations of the Nomenclature Committee on Cell Death. Cell Death Differ. 19:107-120.

Glick D, Barth S, Macleod KF, (2010). Autophagy: cellular and molecular mechanisms. J Pathol. 221:3-12.

Goldsmith MR, Shimada T, Abe H, (2005). The genetics and genomics of the silkworm, *Bombyx mori*. Annu Rev Entomol. 50:71-100.

Gullan PJ and Cranston PS, (2014). The insects - An outline of entomology. Fifth edition. Wiley-Blackwell. ISBN: 978-1-118-84615-5.

Guo E, He Q, Liu S, Tian L, Sheng Z et al., (2012). MET is required for the maximal action of 20-hydroxyecdysone during *Bombyx* metamorphosis. PLoS ONE. 7:12.

Hailey DW, Rambold AS, Satpute-Krishnan P, Mitra K, Sougrat R et al., (2010). Mitochondria supply membranes for autophagosome biogenesis during starvation. Cell. 141:656-667.

Hakim RS, Baldwin K, Smagghe G., (2010). Regulation of midgut growth, development and metamorphosis. Annu Rev Entomol. 55:593-608.

Hamasaki M, Furuta N, Matsuda A, Nezu A, Yamamoto A et al., (2013). Autophagosomes form at ER-mitochondria contact sites. Nature. 495:389-393.

Hay BA, Wassarman DA, Rubin GM, (1995). *Drosophila* homologs of baculovirus inhibitor of apoptosis proteins function to block cell death. Cell. 83:1253-1262.

Hayashi-Nishino M, Fujita N, Noda T, Yamaguchi A, Yoshimori T et al., (2009). A subdomain of the endoplasmic reticulum forms a

cradle for autophagosome formation. Nat Cell Biol. 11:1433-1437.

Hu C, Zhang X, Teng YB, Hu HX, Li WF, (2010). Structure of autophagy-related protein Atg8 from the silkworm *Bombyx mori*. Acta Crystallogr Sect F Struct Biol Cryst Commun. 66:787-790.

Huh JR, Vernooy SY, Yu H, Yan N, Shi Y et al., (2004). Multiple apoptotic caspase cascades are required in nonapoptotic roles for *Drosophila* spermatid individualization. PLoS Biol. 2:e15.

Ichimura Y, Kirisako T, Takao T, Satomi Y, Shimonishi Y et al., (2000). A ubiquitin-like system mediates protein lipidation. Nature. 408:488–492.

Itakura E, Mizushima N, (2010). Characterization of autophagosome formation site by a hierarchical analysis of mammalian Atg proteins. Autophagy. 6:764-776.

Jiang C, Lamblin AF, Steller H, Thummel CS, (2000). A steroid-triggered transcriptional hierarchy controls salivary gland cell death during *Drosophila* metamorphosis. Mol Cell. 5:445–455.

Johansen T, Lamark T, (2011). Selective autophagy mediated by autophagic adapter proteins. Autophagy. 7:279-296.

Jürgensmeier JM, Xie Z, Deveraux Q, Ellerby, L, Bredesen D et al., (1998). Bax directly induces release of cytochrome c from isolated mitochondria. Proc Nat Acad Sci USA. 95:4997-5002.

Kabeya Y, Mizushima N, Ueno T, Yamamoto A, Kirisako T et al., (2000). LC3, a mammalian homologue of yeast Apg8p, is localized in autophagosome membranes after processing. EMBO J. 19:5720-5728.

Kabeya Y, Mizushima N, Yamamoto A, Oshitani-Okamoto S, Ohsumi Y et al., (2004). LC3, GABARAP and GATE16 localize to autophagosomal membrane depending on form-II formation. J Cell Sci. 117:2805-2812.

Kanki T, Wang K, Cao Y, Baba M, Klionsky DJ, (2009). Atg32 is a mitochondrial protein that confers selectivity during mitophagy. Dev Cell. 17:98-109.

Kauppila S, Maaty WS, Chen P, Tomar RS, Eby MT et al., (2003). Eiger and its receptor, Wengen, comprise a TNF-like system in *Drosophila*. Oncogene. 22:4860-4867.

Kaushal GP, (2012). Autophagy protects proximal tubular cells from injury and apoptosis. Kidney Int. 82:1250-1253.

Kessel DH, Price M, Reiners JJ, (2012). ATG7 deficiency suppresses apoptosis and cell death induced by lysosomal photodamage. Autophagy. 8:1333–1341.

Khoa DB, Takeda M, (2012). Expression of autophagy 8 (Atg8) and its role in the midgut and other organs of the greater wax moth, *Galleria mellonella*, during metamorphic remodelling and under starvation. Insect Mol Biol. 21:473-487.

Khoa DB, Trang LT, Takeda M, (2012). Expression analyses of caspase-1 and related activities in the midgut of *Galleria mellonella* during metamorphosis. Insect Mol Biol. 21:247-256.

Kilpatrick ZE, Cakouros D, Kumar S, (2005). Ecdysone-mediated up-regulation of the effector caspase DRICE is required for hormone-dependent apoptosis in *Drosophila* cells. J Biol Chem. 280:11981–11986.

Kirisako T, Ichimura Y, Okada H, Kabeya Y, Mizushima N et al., (2000). The reversible modification regulates the membrane-binding state of Apg8/Aut7 essential for autophagy and the cytoplasm to vacuole targeting pathway. J Cell Biol. 151:263–276

Kissova I, Deffieu M, Manon S, Camougrand N, (2004). Uth1p is involved in the autophagic degradation of mitochondria. J Biol Chem. 279:39068-39074.

Klionsky DJ, Abdalla FC, Abeliovich H, Abraham RT, Acevedo-Arozena A et al., (2012). Guidelines for the use and

interpretation of assays for monitoring autophagy. Autophagy. 8:445-544.

Kroemer G, Galluzzi L, Vandenabeele P, Abrams J, Alnemri ES et al., (2009). Classification of cell death: recommendations of the Nomenclature Committee on Cell Death. Cell Death Differ. 16: 3-11.

Kroemer G, Levine B, (2008). Autophagic cell death: the story of a misnomer. Nat Rev Mol Cell Biol. 9:1004-1010.

Kumar S, Doumanis J, (2000). The fly caspases. Cell Death Differ. 7:1039–1044.

Lai YK, Hsu JT, Chu CC, Chang TY, Pan KL et al., (2012). Enhanced recombinant protein production and differential expression of molecular chaperones in sf-caspase-1-repressed stable cells after baculovirus infection. BMC Biotechnol. 12:83.

Lee CY, Wendel DP, Reid P, Lam G, Thummel CS et al., (2000). E93 directs steroid-triggered programmed cell death in *Drosophila*. Mol Cell. 6:433–443.

Leulier F, Rodriguez A, Khush RS, Abrams JM, Lemaitre B, (2000). The *Drosophila* caspase Dredd is required to resist gram-negative bacterial infection. EMBO Rep. 1:353–358.

Li K, Guo E, Hossain MS, Li Q, Cao Y et al., (2015). *Bombyx* E75 isoforms display stage- and tissue-specific responses to 20-hydroxyecdysone. Sci Rep. 5:12114.

Li Q, Deng X, Yang W, Huang Z, Tettamanti G et al., (2010). Autophagy, apoptosis, and ecdysis-relatedgene expression in the silk gland of the silkworm (*Bombyx mori*) during metamorphosis. Can J Zool. 88:1169–1178.

Li WW, Li J, Bao JK, (2012). Microautophagy: lesser-known self-eating. Cell Mol Life Sci. 69:1125-1136.

Liu Q, Chejanovsky N, (2006). Activation pathways and signal-mediated upregulation of the insect *Spodoptera frugiperda* caspase-1. Apoptosis. 11:487-496.

Liu Q, Qi Y, Chejanovsky N, (2005). *Spodoptera littoralis* caspase-1, a Lepidopteran effector caspase inducible by apoptotic signaling. Apoptosis. 10:787-795.

Liu R, Zhi X, Zhong Q, (2015). ATG14 controls SNARE-mediated autophagosome fusion with a lysosome. Autophagy. 11:847-849.

Liu X, Dai F, Guo E, Li K, Ma L et al., 2015. 20-Hydroxyecdysone (20E) Primary Response Gene E93 Modulates 20E signaling to Promote Bombyx Larval-Pupal Metamorphosis. J Biol Chem. 290:27370-27383.

Luo X, Budihardjo I, Zou H, Slaughter C, Wang X, (1998). Bid, a Bcl2 interacting protein, mediates cytochrome c release from mitochondria in response to activation of cell surface death receptors. Cell. 94:481-490.

Malagoli D, Abdalla FC, Cao Y, Feng Q, Fujisaki K et al., (2010). Autophagy and its physiological relevance in arthropods: current knowledge and perspectives. Autophagy. 5:575-588.

Manaboon M, Iga M, Sakurai S, (2008). Nongenomic and genomic actions of an insect steroid coordinately regulate programmed cell death of anterior silk glands of *Bombyx mori*. Invertebrate Surviv J. 5:1–22.

Mariño G, Niso-Santano M, Baehrecke EH, Kroemer G. (2014) Self-consumption: the interplay of autophagy and apoptosis. Nat Rev Mol Cell Biol. 5:81-94.

Martin SJ, Reutelingsperger CP, McGahon AJ, Rader JA, van Schie RC et al., (1995). Early redistribution of plasma membrane phosphatidylserine is a general feature of apoptosis regardless of the initiating stimulus: inhibition by overexpression of Bcl-2 and Abl. J Exp Med. 182:1545-1556.

Matsui H, Kakei M, Iwami M, Sakurai S, (2012). Hormonal regulation of the death commitment in programmed cell death

of the silkworm anterior silk glands. J Insect Physiol. 58:1575-1581.

Meier P, Finch A, Evan G, (2000). Apoptosis in development. Nature. 407:796-801.

Mizushima N, (2005). The pleiotropic role of autophagy: From protein metabolism to bactericide. Cell Death Differ. 12:1535-1541.

Mizushima N, (2010). The role of the Atg1/ULK1 complex in autophagy regulation. Curr Opin Cell Biol. 22:132-139.

Moss DK, Betin, VM, Malesinski SD, Lane JD, (2006). A novel role for microtubules in apoptotic chromatin dynamics and cellular fragmentation. J Cell Sci. 119:2362-2374.

Moss WD, (1983). Acid phosphatases. In: Bergmeyer J., Grassi M. (Eds). Esterases, glycosidases, lyases, ligases. Vol. 4: Methods of enzymatic analysis. Verlag-Chemie, Weinheim: 92-106.

Mpakou VE, Nezis IP, Stravopodis DJ, Margaritis LH, Papassideri IS, (2006). Programmed cell death of the ovarian nurse cells during oogenesis of the silkmoth *Bombyx mori*. Dev Growth Differ. 48:419-428.

Müller F, Adori C, Sass M, (2004). Autophagic and apoptotic features during programmed cell death in the fat body of the tobacco hornworm (*Manduca sexta*). Eur J Cell Biol. 83:67-78.

Muro I, Berry DL, Huh JR, Chen CH, Huang H et al., (2006). The *Drosophila* caspase Ice is important for many apoptotic cell deaths and for spermatid individualization, a nonapoptotic process. Development. 133:3305–3315.

Nazio F, Strappazzon F, Antonioli M, Bielli P, Cianfanelli V et al., (2013). mTOR inhibits autophagy by controlling ULK1 ubiquitylation, self-association and function through AMBRA1 and TRAF6. Nat Cell Biol. 15:406-416.

Nezis IP, Shravage BV, Sagona AP, Lamark T, Bjørkøy G et al., (2010). Autophagic degradation of dBruce controls DNA

fragmentation in nurse cells during late *Drosophila* melanogaster oogenesis. J Cell Biol. 190:523-531.

Oral O, Oz-Arslan D, Itah Z, Naghavi A, Deveci R et al., (2012). Cleavage of Atg3 protein by caspase-8 regulates autophagy during receptor-activated cell death. Apoptosis. 17:810–820.

Ou J, Deng HM, Zheng SC, Huang LH, Feng QL et al., (2014). Transcriptomic analysis of developmental features of *Bombyx mori* wing disc during metamorphosis. BMC Genomics. 15:820.

Papinski D, Schuschnig M, Reiter W, Wilhelm L, Barnes CA, (2014). Early steps in autophagy depend on direct phosphorylation of Atg9 by the Atg1 kinase. Mol Cell. 53:471-483.

Parthasarathy R, Palli SR, (2007). Developmental and hormonal regulation of midgut remodeling in a lepidopteran insect, *Heliothis virescens*. Mech Dev. 124:23-34.

Pattingre S, Tassa A, Qu X, Garuti R, Liang XH et al., (2005). Bcl-2 antiapoptotic proteins inhibit Beclin 1-dependent autophagy. Cell. 122:927-939.

Rao L, Perez D, White E, (1996). Lamin proteolysis facilitates nuclear events during apoptosis.. J Cell Biol. 135:1441–1455.

Reddy RM, Prasad GV, (2011). Silk - the prospective and compatible bio-material for advanced functional applications. Trends Appl Sci Res. 6:89-95.

Rees HH, (1995). Ecdysteroid biosynthesis and inactivation in relation to function. Eur J Entomol. 92:9-39.

Reggiori F and Klionsky DJ, (2002). Autophagy in the Eukaryotic Cell. Eukaryot Cell. 1:11-21.

Riedl SJ, Shi Y, (2004). Molecular mechanisms of caspase regulation during apoptosis. Nat Rev Mol Cell Biol. 5:897-907.

Roe R.M., Venkatesh K, (1990). Metabolism of juvenile hormones: degradation and titer regulation. in: A.P. Gupta (Ed.), Morphogenetic Hormones of Arthropods, vol. IRutgers University Press, New Brunswick, pp. 126-179.

Romanelli D, Casati B, Franzetti E, Tettamanti G, (2014). A molecular view of autophagy in Lepidoptera. Biomed Res Int. 2014:902315.

Rubinstein AD, Eisenstein M, Ber Y, Bialik S, Kimchi A, (2011). The autophagy protein Atg12 associates with antiapoptotic Bcl-2 family members to promote mitochondrial apoptosis. Mol Cell. 44:698–709.

Rusten TE, Lindmo K, Juhász G, Sass M, Seglen PO et al., (2004). Programmed autophagy in the *Drosophila* fat body is induced by ecdysone through regulation of the PI3K pathway. Dev Cell. 7:179-192.

Satake S, Kaya M, Sakurai S et al., (1998). Hemolymph ecdysteroid titer and ecdysteroid-dependent developmental events in the last-larval stadium of the silkworm, *Bombyx mori*: role of low ecdysteroid titer in larval-pupal metamorphosis and a reappraisal of the head critical period. J Insect Physiol. 44:867-881.

Sass M, Kovacs J, (1975). Ecdysterone and an analogue of juvenile hormone on the autophagy in the cells of fat body of *Mamestra brassicae*. Acta Biol Acad Sci Hung. 26:189-196.

Scott RC, Juhász G, Neufeld TP, (2007). Direct induction of autophagy by Atg1 inhibits cell growth and induces apoptotic cell death. Curr Biol. 17:1-11.

Sekimoto T, Iwami M, Sakurai S, (2006). Coordinate responses of transcription factors to ecdysone during programmed cell death in the anterior silk gland of the silkworm, *Bombyx mori*. Insect Mol Biol. 15:281–292.

Shiozaki EN, Chai J, Shi Y, (2002). Oligomerization and activation of caspase-9, induced by Apaf-1 CARD. Proc Natl Acad Sci USA. 99:4197-4202.

Shpilka T, Weidberg H, Pietrokovski S, Elazar Z, (2011). Atg8: an autophagy-related ubiquitin-like protein family. Genome Biol. 12:226.

Silva MT, (2010). Secondary necrosis: the natural outcome of the complete apoptotic program. FEBS Lett. 584:4491-4499.

Stevens J, Dunse K, Fox J, Evans S and Anderson M, (2012). Biotechnological Approaches for the Control of Insect Pests in Crop Plants, Pesticides - Advances in Chemical and Botanical Pesticides, Dr. R.P. Soundararajan (Ed.), ISBN: 978-953-51-0680-7, InTech.

Stoven S, Silverman N, Junell A, Hedengren-Olcott M, et al., (2003). Caspase-mediated processing of the *Drosophila* NF-kappaB factor Relish. Proc Natl Acad Sci USA. 100:5991-5996.

Suzuki K, Kubota Y, Sekito T, Ohsumi Y, (2007). Hierarchy of Atg proteins in pre-autophagosomal structure organization. Genes Cells. 12:209-218.

Tasdemir E, Maiuri MC, Galluzzi L, Vitale I, Djavaheri-Mergny M et al., (2008). Regulation of autophagy by cytoplasmic p53. Nat Cell Biol. 10:676–687.

Taylor RC, Cullen SP, Martin SJ, (2008). Apoptosis: controlled demolition at the cellular level. Nat Rev Mol Cell Biol. 9:231-241.

Tazima Y, (1978). The silkworm: an important laboratory tool. Ed. Kodanska, Tokio.

Tenev T, Zachariou A, Wilson R, Ditzel M, Meier P, (2004). IAPs are functionally non-equivalent and regulate effector caspases through distinct mechanisms. Nat Cell Biol. 7:70-77.

Teng X, Zhang Z, He G, Yang L, Li F, (2012). Validation of reference genes for quantitative expression analysis by real-time rt-PCR in four lepidopteran insects. J Insect Sci. 12:60.

Terashima J, Yasuhara N, Iwami M, Sakurai S, Sakurai S, (2000). Programmed cell death triggered by insect steroid hormone, 20-

hydroxyecdysone, in the anterior silk gland of the silkworm, *Bombyx mori*. Dev Genes Evol. 210:545-558.

Terra WR, (2001). The origin and functions of the insect peritrophic membrane and peritrophic gel. Arch Insect Biochem Physiol. 47:47-61.

Tettamanti G, Grimaldi A, Casartelli M, Ambrosetti E, Ponti B et al., (2007). Programmed cell death and stem cell differentiation are responsible for midgut replacement in *Heliothis virescens* during prepupal instar. Cell Tissue Res. 330:345-359.

Tian L, Liu S, Liu H, Li S, (2012). 20-hydroxyecdysone upregulates apoptotic genes and induces apoptosis in the *Bombyx* fat body. Arch Insect Biochem Physiol. 79:207-219.

Tian L, Ma L, Guo E, Deng X, Ma S et al., (2013). 20-hydroxyecdysone upregulates Atg genes to induce autophagy in the *Bombyx* fat body. Autophagy. 9:1172–1187.

Tooze SA, Yoshimori T, (2010). The origin of the autophagosomal membrane. Nat Cell Biol. 12:831-835.

Truman JW and Riddiford LM, (1999). The origins of insect metamorphosis. Nature. 401:447-452.

Truman JW and Riddiford LM, (2002). Endocrine insights into the evolution of metamorphosis in insects. Ann Rev Entomol. 47:467-500.

Ura S, Masuyama N, Graves JD, Gotoh Y et al., (2001). Caspase cleavage of MST1 promotes nuclear translocation and chromatin condensation. Proc Natl Acad Sci USA. 98:10148–10153.

Uwo MF, Ui-Tei K, Park P, Takeda M, (2002). Replacement of midgut epithelium in the greater wax moth, *Galleria mellonella*, during larval-pupal moult. Cell Tissue Res. 308:319-331.

Wang CW, Klionsky DJ, (2004). Microautophagy. In Autophagy (ed. DJ.Klionsky), pp. 107-114. Georgetown: Landes Bioscience.

Wang J, Xia Q, He X, Dai M, Ruan J et al., (2005). SilkDB: a knowledgebase for silkworm biology and genomics. Nucleic Acids Res. 33: D399-402.

Wei Y, Pattingre S, Sinha S, Bassik M, Levine B, (2008). JNK1-mediated phosphorylation of Bcl-2 regulates starvation-induced autophagy. Mol Cell. 30:678–688.

Welinder C, Ekblad L, (2011). Coomassie staining as loading control in Western blot analysis. J Proteome Res. 10:1416–1419.

Wigglesworth VB, (1972). Digestion and nutrition. In: The principles of insect physiology. Chapman & Hall, London, pp 476-552.

Wirawan E, Vande Walle L, Kersse K, Cornelis S, Claerhout S et al., (2010). Caspase-mediated cleavage of Beclin-1 inactivates Beclin-1-induced autophagy and enhances apoptosis by promoting the release of proapoptotic factors from mitochondria. Cell Death Dis. 1:e18.

Wu W, Wei W, Ablimit M, Ma Y, Fu T et al., (2011). Responses of two insect cell lines to starvation: autophagy prevents them from undergoing apoptosis and necrosis, respectively. J Insect Physiol. 57:723-734.

Wu YT, Tan HL, Shui G, Bauvy C, Huang Q et al., (2010) . Dual role of 3-methyladenine in modulation of autophagy via different temporal patterns of inhibition on class I and III phosphoinositide 3-kinase. J Biol Chem. 285:10850-10861.

Xia Q, Li S, Feng Q, (2014). Advances in silkworm studies accelerated by the genome sequencing of *Bombyx mori*. Annu Rev Entomol. 59:513-536.

Xu D, Wang Y, Willecke R, Chen Z, Ding T et al., (2006). The effector caspases drICE and dcp-1 have partially overlapping functions in the apoptotic pathway in *Drosophila*. Cell Death Differ. 13:1697–1706.

Yacobi-Sharon K, Namdar Y, Arama E, (2013). Alternative germ cell death pathway in *Drosophila* involves HtrA2/Omi, lysosomes, and a caspase-9 counterpart. Dev Cell. 25:29–42.

Yang X, Chang HY, Baltimore D, (1998). Essential role of CED-4 oligomerization in CED-3 activation and apoptosis. Science. 281:1355–1357.

Yin VP, Thummel CS, (2004). A balance between the diap1 death inhibitor and reaper and hid death inducers controls steroid-triggered cell death in *Drosophila*. Proc Natl Acad Sci USA. 101:8022-8027.

Ylä-Anttila P, Vihinen H, Jokitalo E, Eskelinen EL, (2009). 3D tomography reveals connections between the phagophore and endoplasmic reticulum. Autophagy. 5:1180-1185.

Youle RJ, Narendra DP, (2011). Mechanisms of mitophagy. Nat Rev Mol Cell Biol. 12:9-14.

Young MM, Takahashi Y, Khan O, Park S, Hori T et al., (2012). Autophagosomal membrane serves as platform for intracellular death-inducing signaling complex (iDISC)-mediated caspase-8 activation and apoptosis. J Biol Chem. 287:12455-12468.

Yousefi S, Perozzo R, Schmid I, Ziemiecki A, Schaffner T et al., (2006). Calpain-mediated cleavage of Atg5 switches autophagy to apoptosis. Nat Cell Biol. 8:1124–1132.

Yu X, Wang L, Acehan D, Wang X, Akey CW, (2006). Three-dimensional structure of a double apoptosome formed by the *Drosophila* Apaf-1 related killer. J Mol Biol. 355:577–589.

Yuan S, Yu X, Topf M, Dorstyn L, Kumar S et al., (2011). Structure of the *Drosophila* apoptosome at 6.9 a resolution. Structure. 19:128–140.

Zhang JY, Pan MH, Sun ZY, Huang SJ, Yu ZS et al., (2010). The genomic underpinnings of apoptosis in the silkworm*, Bombyx mori*. BMC Genomics. 11:611.

Zhang X, Hu ZY, Li WF, Li QR, Deng XJ et al., (2009). Systematic cloning and analysis of autophagy-related genes from the silkworm *Bombyx mori*. BMC Mol Biol. 10:50.

Zhang XJ, Chen S, Huang KX, Le WD, (2013). Why should autophagic flux be assessed?. Acta Pharmacol Sin. 34:595-599.

Zirin J, Cheng D, Dhanyasi N, Cho J, Dura JM et al., (2013). Ecdysone signaling at metamorphosis triggers apoptosis of *Drosophila* abdominal muscles. Dev Biol. 383:275-284.

7 FIGURES

Figure 8 - Expression of *ATG* genes increases during metamorphosis. qRT-PCR analysis of *BmATG8* (A) and *BmATG1* (B) mRNA levels in midgut tissues during metamorphosis.
Values represent mean ± SEM (**, $p<0.01$ compared to L5D2).

A

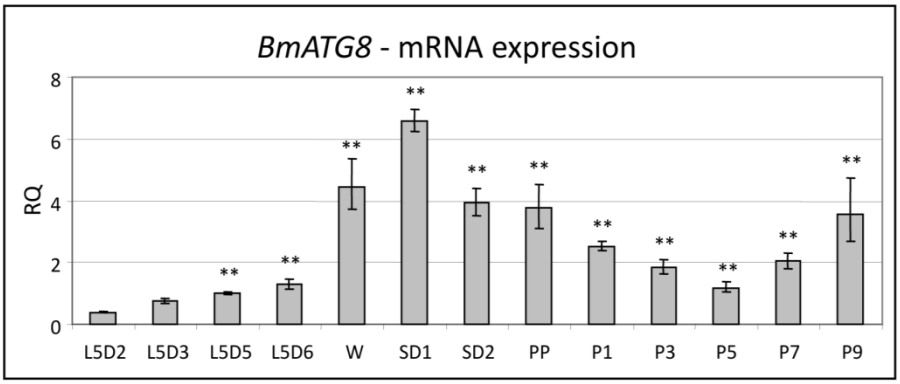
BmATG8 - mRNA expression
RQ
0
2
4
6
8
**
L5D2
L5D3
L5D5
L5D6
W
SD1
SD2
PP
P1
P3
P5
P7
P9

B

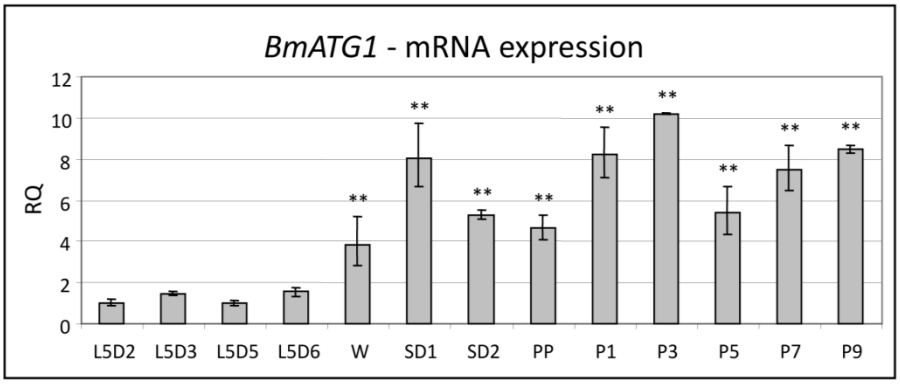
BmATG1 - mRNA expression
RQ
0
2
4
6
8
10
12
**
L5D2
L5D3
L5D5
L5D6
W
SD1
SD2
PP
P1
P3
P5
P7
P9

Figure 9 - Autophagy is activated during the spinning stage. (A) Amino acid sequence alignment of BmAtg8 with HsGabarap; (B) western blot analysis of BmAtg8 on BL21DE3/pET28+BmAtg8 bacteria (+), BL21DE3/pET28 bacteria (-) and silkworm midgut tissues (m), by using anti-HsGabarap antibody; (C) western blot analysis of BmATG8-PE expression during metamorphosis; (D, E) immunofluorescence staining of BmAtg8 showing the presence of autophagosomes (arrows) in midgut tissues at L5D5 (D) and SD2 (E) stage; (F) TEM images of autophagosomes in midgut cells at SD2 stage (a: autophagosome; arrows: autophagosome membrane); (G) analysis of acid phosphatase activity in midgut. Values represent mean ± SEM (**, $p<0.01$ compared to L5D2).

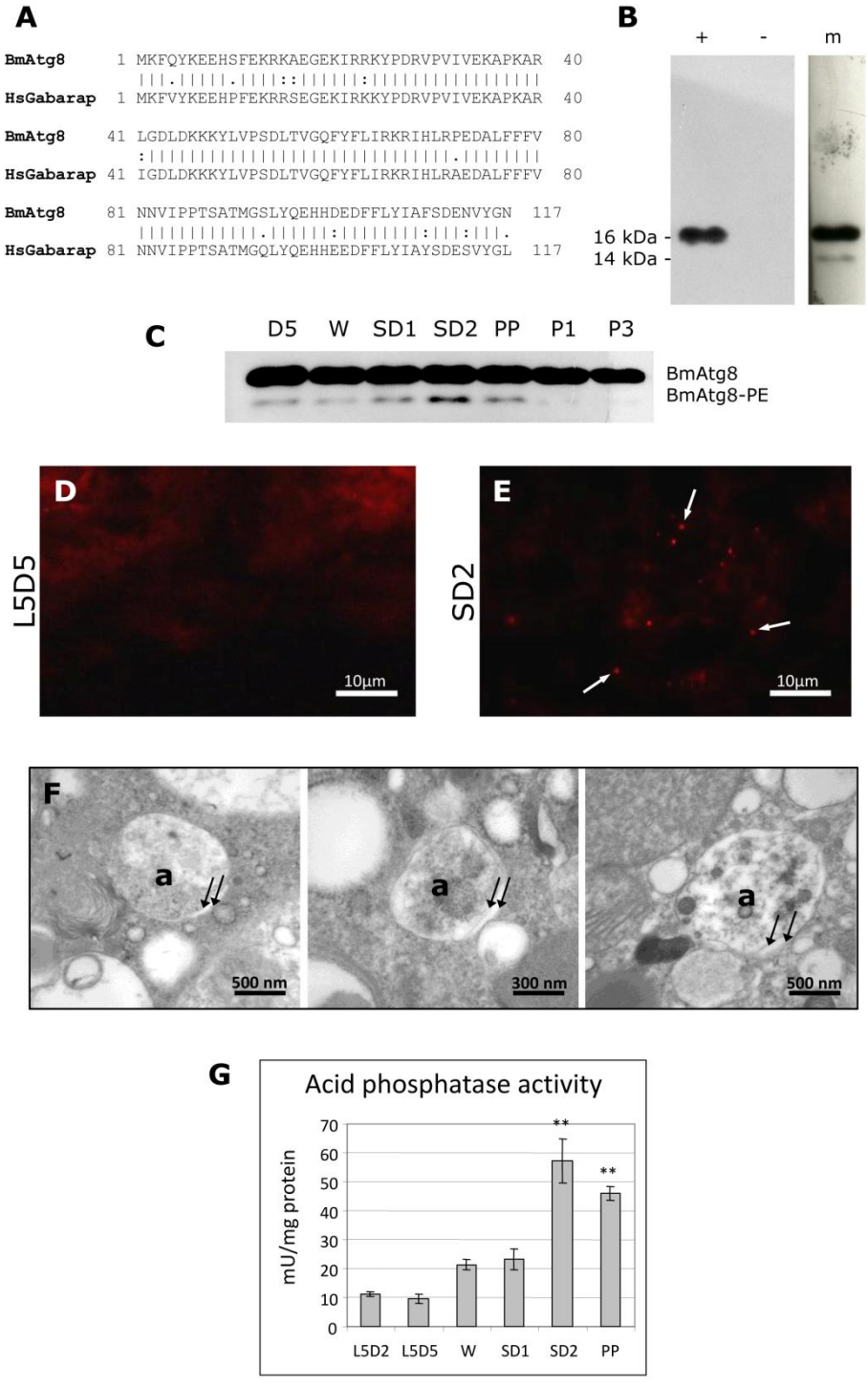
A
BmAtg8 1 MKFQYKEEHSFEKRKAEGEKIRRKYPDRVPVIVEKAPKAR 40
HsGabarap 1 MKFVYKEEHPFEKRRSEGEKIRKKYPDRVPVIVEKAPKAR 40
BmAtg8 41 LGDLDKKKYLVPSDLTVGQFYFLIRKRIHLRPEDALFFFV 80
HsGabarap 41 IGDLDKKKYLVPSDLTVGQFYFLIRKRIHLRAEDALFFFV 80
BmAtg8 81 NNVIPPTSATMGSLYQEHHDEDFFLYIAFSDENVYGN 117
HsGabarap 81 NNVIPPTSATMGQLYQEHHEEDFFLYIAYSDESVYGL 117
B
+
-
m
16 kDa -
14 kDa -
C
D5 W SD1 SD2 PP P1 P3
BmAtg8
BmAtg8-PE
D
L5D5
10µm
E
SD2
10µm
F
a
500 nm
a
300 nm
a
500 nm
G
Acid phosphatase activity
mU/mg protein
70
60
50
40
30
20
10
0
**
**
L5D2 L5D5 W SD1 SD2 PP

Figure 10 - Apoptosis is activated during larval-pupal transition. (A, B) qRT-PCR analysis of *BmCASPASE-1* (A) and *BmCASPASE-5* (B); (C) amino acid sequence alignment of BmCaspase-1 with HsCaspase-3 showing the conservation of the "EDT" cleavage site recognized by the anti-cleaved Caspase-3 antibody; (D, E) western blot analysis of cleaved (D) and uncleaved (E) BmCaspase-1 during metamorphosis.
Values represent mean ± SEM (*, $p<0.05$; **, $p<0.01$ compared to L5D2).

A

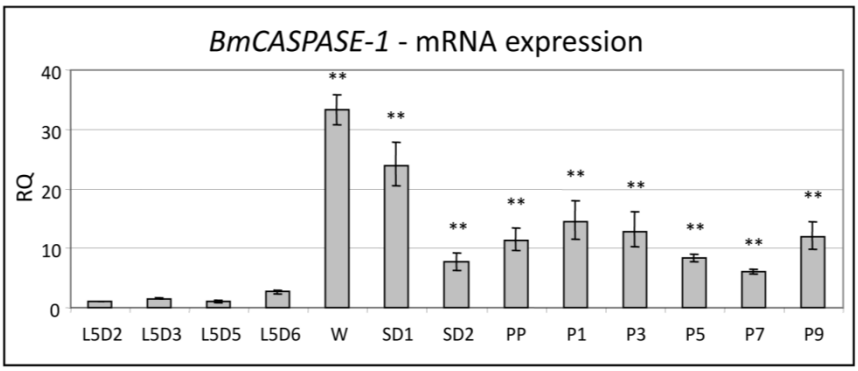

B

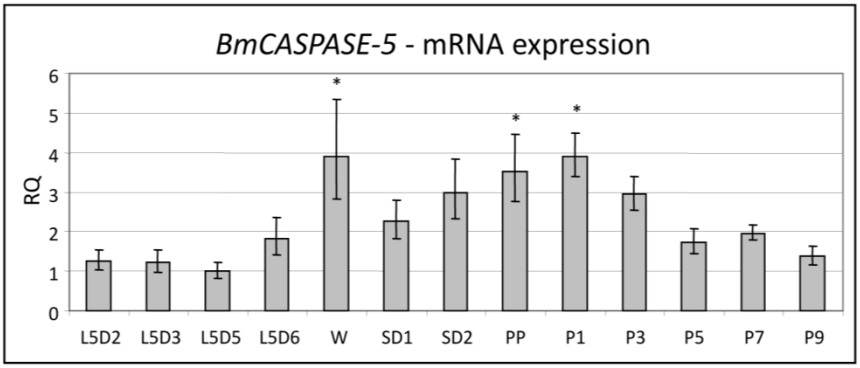

C

BmCaspase-1 CQGDKLDGGITLSNT**ETD** 192
HsCaspase-3 CRGTELDCGI-----**EDT** 175

D

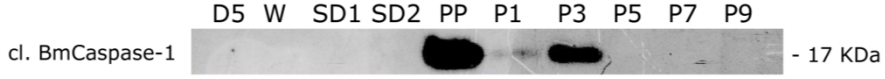

E

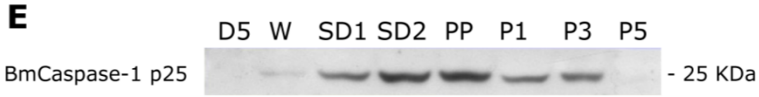

Figure 11 - Yellow body cells undergo secondary necrosis. (A) SEM image showing ruptures (arrows) in the membrane of the yellow body cells; (B) analysis of the release of cleaved BmCaspase-1 from the yellow body cells (P3 stage). The active caspase is detected both in the luminal space (l) and in the yellow body cells (c).

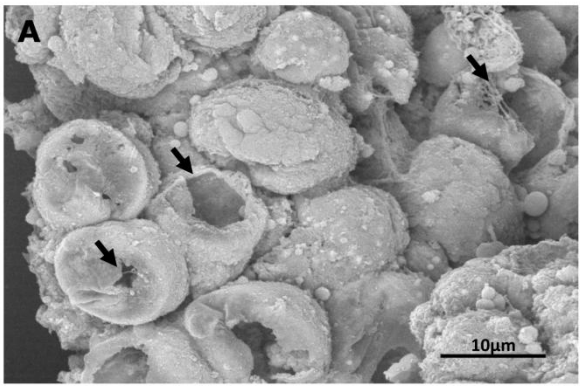
A
10µm

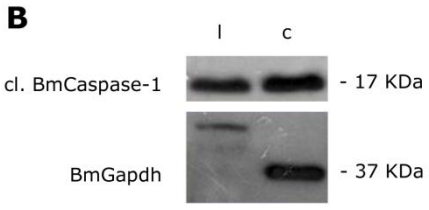
B
I
c
cl. BmCaspase-1
- 17 KDa
BmGapdh
- 37 KDa

Figure 12 - Autophagy is activated by 20E. (A, B) qRT-PCR analysis of *BmATG8* (A) and *BmATG1* (B) in midgut cells after administration of 20E; (C, D) western blot analysis of BmAtg8-PE (C) and acid phosphatase activity (D) in midgut of larvae injected with the hormone; (E) western blot analysis of p-Bm4ebp1 in hormone-treated larvae.
Values represent mean ± SEM (**, $p<0.01$).

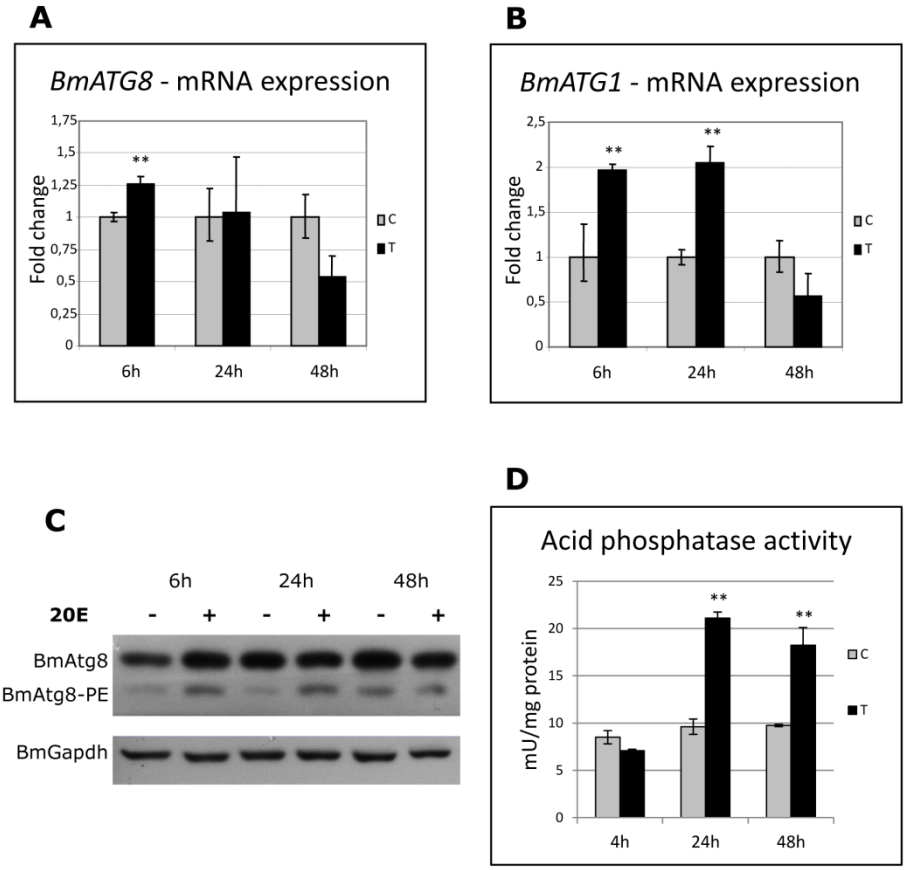
A
BmATG8 - mRNA expression
Fold change
1,75
1,5
1,25
1
0,75
0,5
0,25
0
**
C
T
6h
24h
48h
B
BmATG1 - mRNA expression
Fold change
2,5
2
1,5
1
0,5
0
**
**
C
T
6h
24h
48h
C
6h
24h
48h
20E
- + - + - +
BmAtg8
BmAtg8-PE
BmGapdh
D
Acid phosphatase activity
mU/mg protein
25
20
15
10
5
0
**
**
C
T
4h
24h
48h
E
6h
24h
48h
20E
- + - + - +
p-Bm4ebp1
BmGapdh

Figure 13 - Rapamycin fails to activate a full autophagic response. (A) Western blot analysis of p-Bm4ebp1 in midgut of larvae injected with rapamycin; (B, C) qRT-PCR analysis of *BmATG8* (B) and BmATG1 (C) expression after rapamycin treatment; (D, E) western blot analysis of BmAtg8-PE (D) and acid phosphatase activity (E) after administration of rapamycin.
Values represent mean ± SEM (*, $p<0.05$; **, $p<0.01$).

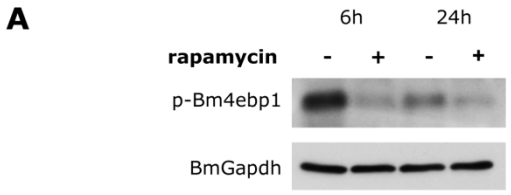
A
6h
24h
rapamycin - + - +
p-Bm4ebp1
BmGapdh

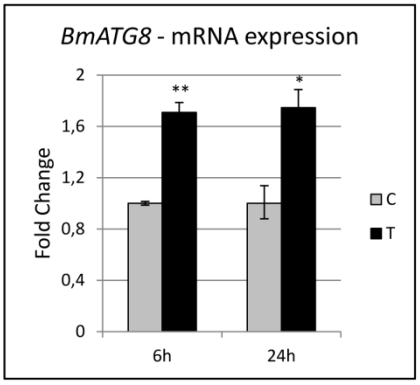
B
BmATG8 - mRNA expression
Fold Change
2
1,6
1,2
0,8
0,4
0
**
*
6h
24h
C
T

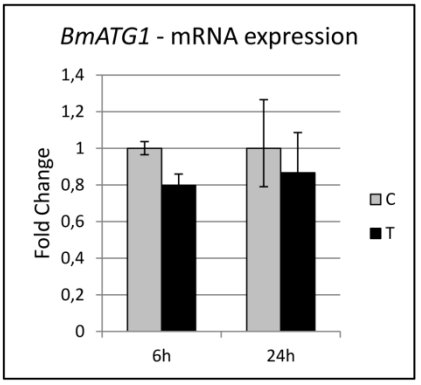
C
BmATG1 - mRNA expression
Fold Change
1,4
1,2
1
0,8
0,6
0,4
0,2
0
6h
24h
C
T

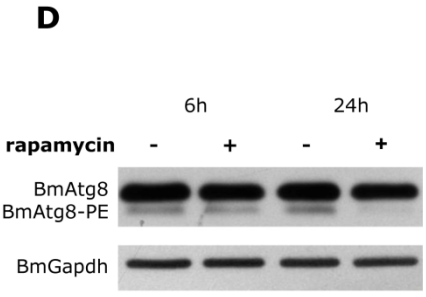
D
6h
24h
rapamycin - + - +
BmAtg8
BmAtg8-PE
BmGapdh

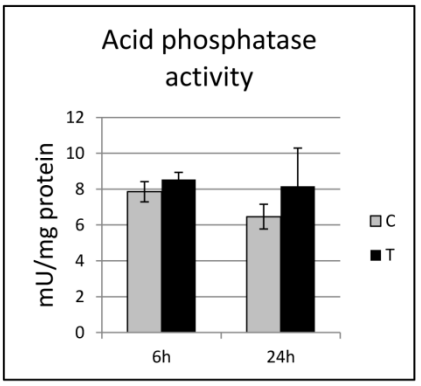
E
Acid phosphatase activity
mU/mg protein
12
10
8
6
4
2
0
6h
24h
C
T

Figure 14 - Apoptosis is activated by 20E. (A, B) qRT-PCR analysis of *BmCASPASE-1* (A) *BmCASPASE-5* (B) in midgut of larvae injected with 20E; (C, D) western blot analysis of cleaved BmCaspase-1 after a single (C) or a double (D) administration of 20E.

Values represent mean ± SEM (**, $p<0.01$).

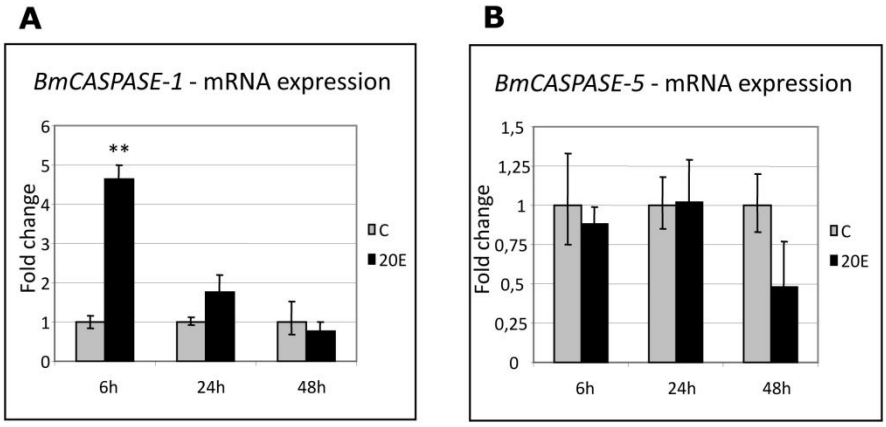
A
BmCASPASE-1 - mRNA expression
Fold change
6
5
4
3
2
1
0
**
C
20E
6h
24h
48h
B
BmCASPASE-5 - mRNA expression
Fold change
1,5
1,25
1
0,75
0,5
0,25
0
C
20E
6h
24h
48h

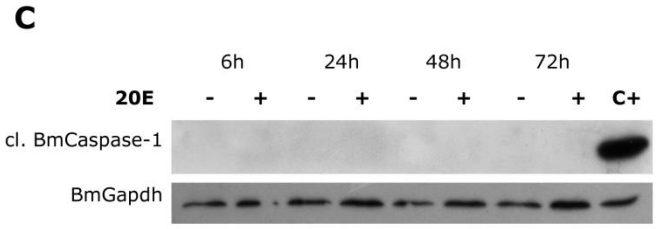
C
6h
24h
48h
72h
20E - + - + - + - + C+
cl. BmCaspase-1
BmGapdh

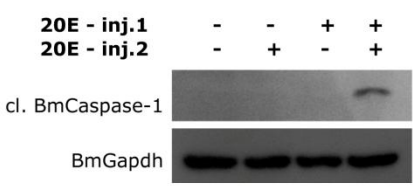
D
20E - inj.1 - - + +
20E - inj.2 - + - +
cl. BmCaspase-1
BmGapdh

Figure 15 - Inhibition of autophagy increases the degeneration of the larval midgut epithelium. (A, B) TEM analysis of midgut cells in control (A) and chloroquine-treated (B) P1 pupae showing a great accumulation of vesicles (arrows) after inhibition of autophagy; (C) Detail of putative autophagosomes in midgut cells of treated larvae; (D, E) western blot analysis of BmAtg8-PE (D) and acid phosphatase activity (E) demonstrating the inhibition of autophagy in midgut cells by chloroquine; (F, G) morphology of larval and pupal epithelium in control (F) and treated (G) pupae; (H) western blot analysis of cleaved BmCaspase-1 in midgut cells of larvae treated with chloroquine. a: autophagosomes; lm: larval midgut epithelium; n: nucleus; pm: pupal epithelium.

Values represent mean ± SEM (*, $p<0.05$).

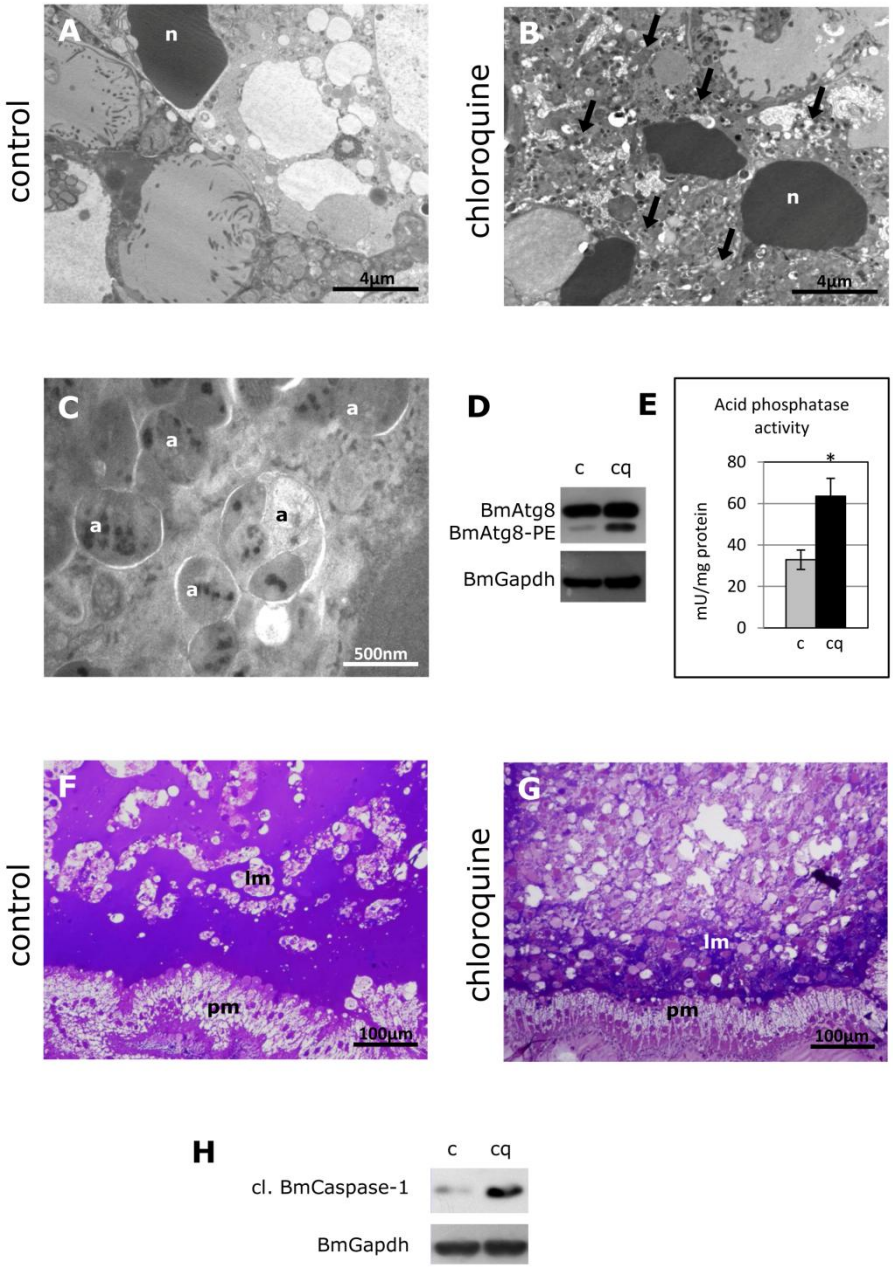
control
A
n
4µm
chloroquine
B
n
4µm
C
a
a
a
a
a
500nm
D
c
cq
BmAtg8
BmAtg8-PE
BmGapdh
E
Acid phosphatase activity
mU/mg protein
80
60
40
20
0
*
c
cq
control
F
lm
pm
100µm
chloroquine
G
lm
pm
100µm
H
c
cq
cl. BmCaspase-1
BmGapdh

Figure 16 - Caspase inhibition delays the degeneration of the larval midgut epithelium. (A-C) Western blot analysis of cleaved BmCaspase-1 in midgut of larvae treated with z.vad.fmk. It is possible to appreciate the dose-dependent inhibition by z.vad.fmk (A), the absence of activated caspase expression in PP, P1 and P3 stages following the administration of the inhibitor at SD2 stage (B) and caspase activation at PP stage despite the injection of the inhibitor at SD1 stage (C); (D, E) TEM analysis of control (D) and treated (E) midgut at PP stage after the administration of z.vad.fmk; (F-I) morphology of larval and pupal epithelium in control (F) and treated (G) P3 pupae; morphology of larval and pupal epithelium in control (H) and treated (I) P9 pupae. lm: larval epithelium; n: nucleus; pm: pupal epithelium; arrows: apoptotic nuclei.

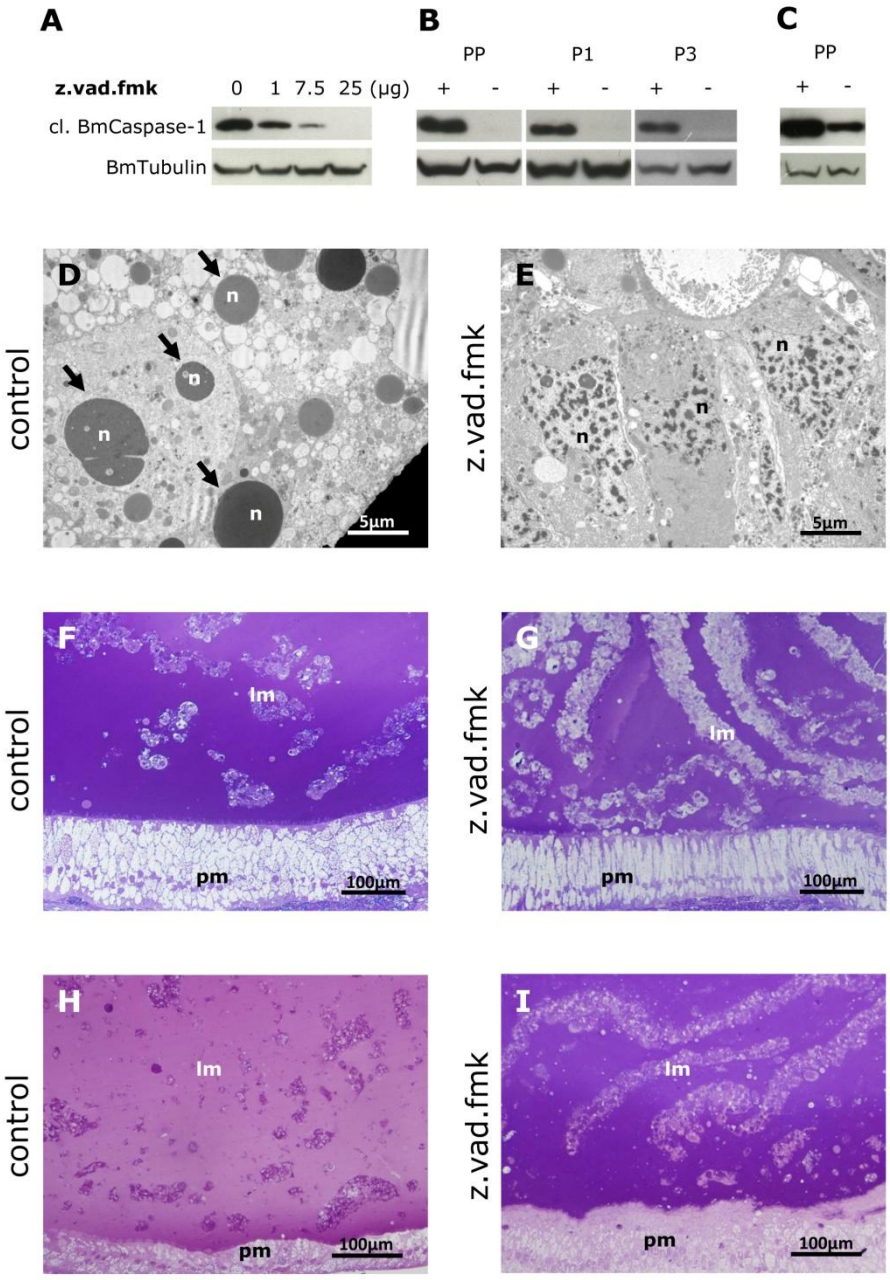
A
B
C
PP
P1
P3
PP
z.vad.fmk
0 1 7.5 25 (µg)
+ - + - + -
+ -
cl. BmCaspase-1
BmTubulin
D
E
control
z.vad.fmk
n
5µm
F
G
lm
pm
100µm
H
I

Figure 17 - Schematic representation of the role and regulation of autophagy and apoptosis during midgut degeneration.

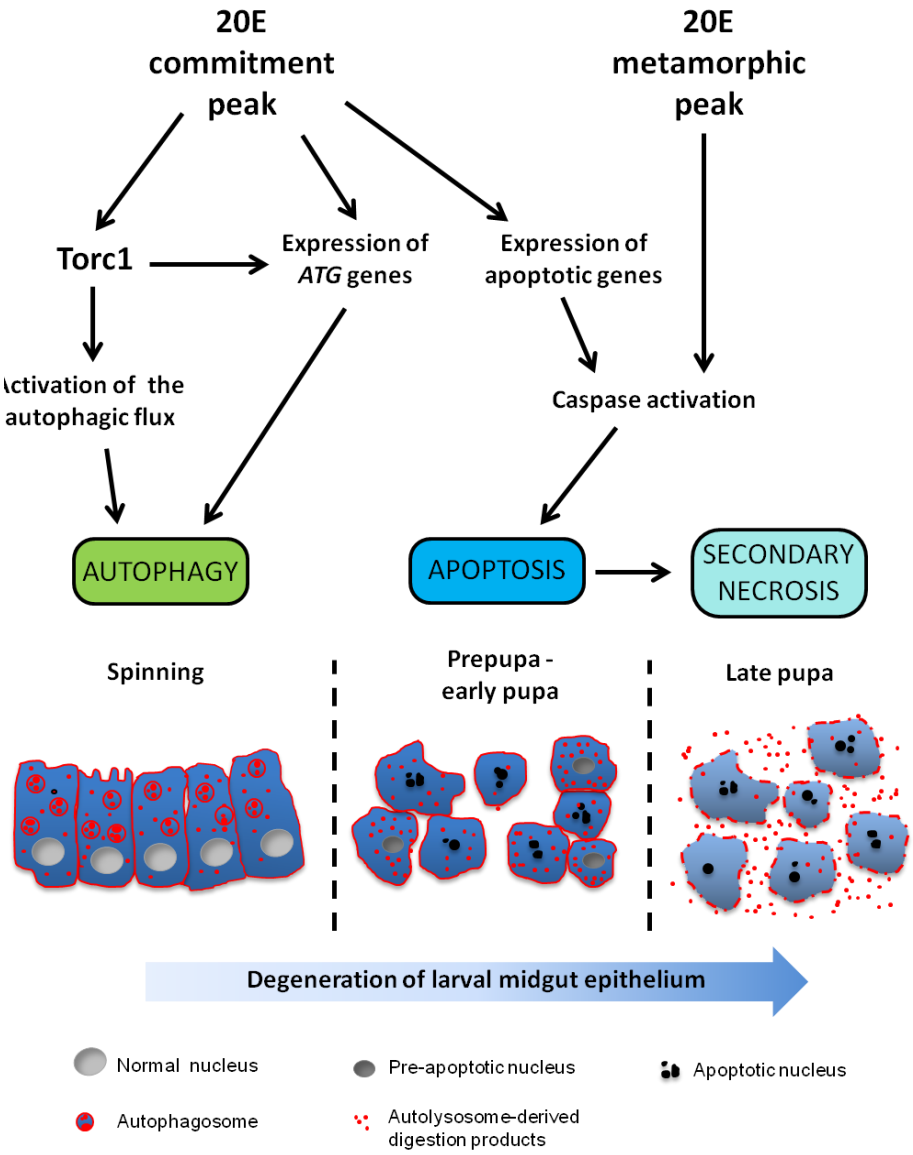
20E commitment peak
20E metamorphic peak
Torc1
Expression of ATG genes
Expression of apoptotic genes
ctivation of the autophagic flux
Caspase activation
AUTOPHAGY
APOPTOSIS
SECONDARY NECROSIS
Spinning
Prepupa - early pupa
Late pupa
Degeneration of larval midgut epithelium
Normal nucleus
Pre-apoptotic nucleus
Apoptotic nucleus
Autophagosome
Autolysosome-derived digestion products